Chair of Nonferrous Metallurgy

Master's Thesis

Strategies for the amelioration of a TBZC intermediate product

Moritz Weitbacher, BSc

March 2022

MONTANUNIVERSITÄT LEOBEN
www.unileoben.ac.at

EIDESSTATTLICHE ERKLÄRUNG

Ich erkläre an Eides statt, dass ich diese Arbeit selbständig verfasst, andere als die angegebenen Quellen und Hilfsmittel nicht benutzt, und mich auch sonst keiner unerlaubten Hilfsmittel bedient habe.

Ich erkläre, dass ich die Richtlinien des Senats der Montanuniversität Leoben zu "Gute wissenschaftliche Praxis" gelesen, verstanden und befolgt habe.

Weiters erkläre ich, dass die elektronische und gedruckte Version der eingereichten wissenschaftlichen Abschlussarbeit formal und inhaltlich identisch sind.

Datum 03.03.2022

Unterschrift Verfasser/in
Moritz Weitbacher

Acknowledgements

The last year was mainly controlled by the Covid 19 pandemic, which often resulted in delays when waiting for analysis data or replacement parts. Therefore, I would like to thank Priv.-Doz. Dr.mont. Stefan Steinlechner for supervising this thesis during these tough times and always being helpful wherever possible. Secondly, having worked on the Chair of Non Ferrous Metallurgy for almost three years now, I want to thank all my colleagues for the pleasant work atmosphere and the constructive environment.

Furthermore, I want to thank my parents Elisabeth Aigner and Veit Czubik for giving me the opportunity of pursuing university education and encouraging me on this journey. Lastly, my gratitude goes out to my girlfriend Beate Schöttner for the prolonged support over the past years and especially during the creation of this thesis as well as proof reading this thesis.

Abstract

This thesis deals with a new process for the hydrometallurgical treatment of iron and zinc containing residues. In a precipitation step, the zinc ideally is extracted from the hydrochloric solution as zinc hydroxide. In a following step, it is then calcinated to ZnO under the formation of steam. In practical experiments, however, it has been observed that the zinc is actually precipitated as a zinc hydroxy chloride compound called tetra basic zinc chloride (TBZC) with the chemical formula $Zn_5(OH)_8Cl_2 \cdot H_2O$. As a consequence, losses of zinc up to 20 % were noticed upon calcination due to the evaporation of $ZnCl_2$. Therefore, in the following different approaches are investigated in order to minimize zinc losses by the selective removal of chlorine.

In this context, two main paths are investigated. On one hand, the thermal route with the options of clinkering and pyrohydrolysis is examined. On the other hand, a hydrometallurgical treatment by the example of soda leaching for the dechlorination of TBZC is looked into. Both routes are evaluated by three steps, with the first step being a literary study on relevant aspects as well as similar residues or intermediate products these treatments are used for. Subsequently, thermodynamic calculations are conducted in FactSage and Hydra in order to gain first insights into the reaction mechanisms at hand. Lastly, these calculations are validated by and compared to lab scale experiments. Additionally, an alternative process path for the precipitation is investigated to prevent the formation of TBZC.

Both the untreated and the already hydrometallurgically treated zinc compound showed a change in appearance upon thermal treatment, losing its pure white color. Since the optical appearance is a major quality aspect for high purity zinc oxide, the causes for this shift in color are also investigated based on literature.

Overall, both routes achieved satisfactory results with a separation of zinc and chlorine of 99 % for pyrohydrolysis in air and 98 % for Soda leaching at 80 °C. However, the results for the less complex setup of clinkering without water vapor only achieved separation of 85 %. Literature and thermodynamic calculations suggest that despite bad practical results, dry thermal treatment is also a promising path for dechlorination. While keeping costs low, higher zinc losses can be expected in parallel.

Kurzfassung

Die vorliegende Arbeit befasst sich mit einem Verfahren zur hydrometallurgischen Aufbereitung von eisen- und zinkhaltigen Rückständen. In einem Fällungsschritt wird das Zink idealerweise als Zinkhydroxid aus der Salzlösung gefällt. In einem weiteren Schritt wird es dann unter Dampfentwicklung zu ZnO kalziniert. In praktischen Experimenten wurde jedoch beobachtet, dass das Zink als Zinkhydroxychloridverbindung mit der Bezeichnung tetrabasisches Zinkchlorid (TBZC) mit der chemischen Formel $Zn_5(OH)_8Cl_2 \cdot H_2O$ ausgefällt wird. Infolgedessen wurden bei der Kalzinierung Zinkverluste von bis zu 20 % aufgrund der Verdampfung von $ZnCl_2$ festgestellt. Daher werden im Folgenden verschiedene Ansätze untersucht, um die Zinkverluste durch die selektive Entfernung von Chlor zu minimieren.

In diesem Zusammenhang werden zwei Hauptkonzepte untersucht. Zum einen wird der thermische Weg betrachtet, mit den Optionen Klinkern und Pyrohydrolyse. Zum anderen wird die hydrometallurgische Behandlung am Beispiel der Sodalaugung zur Entchlorung des TBZC untersucht. Beide Verfahren werden in drei Schritten bewertet, wobei der erste Schritt eine Literaturstudie zu relevanten Aspekten sowie zu ähnlichen Rückständen ist, für die diese Verfahren eingesetzt werden. Anschließend werden thermodynamische Berechnungen in FactSage und Hydra durchgeführt, um erste Einblicke in die jeweiligen Reaktionsmechanismen zu gewinnen. Schließlich werden diese Berechnungen durch Experimente im Labormaßstab validiert und mit diesen verglichen. Darüber hinaus wird eine alternative Route untersucht, mit welcher sich die Fällung von Zink als TBZC verhindern ließe. Während der thermischen Behandlung zeigten sowohl die unbehandelte als auch die bereits hydrometallurgisch behandelte Zinkverbindung eine Farbveränderung und verloren ihre rein weiße Farbe. Da das optische Erscheinungsbild ein wichtiger Qualitätsaspekt für hochqualitatives Zinkoxid ist, wurden auch die Ursachen für diese Farbveränderung anhand der Literatur untersucht.

Insgesamt erzielten beide Verfahren zufriedenstellende Ergebnisse mit einer Trennung zwischen Zink und Chlor auf die beiden Phasen von 99 % bei der Pyrohydrolyse und 98 % bei der Sodalaugung bei 80 °C. In der weniger komplexen Klinkerbehandlung ohne Wasserdampf wurde hingegen nur eine Trennung von 85 % erreicht. Aus Literatur und thermodynamischen Berechnungen geht jedoch hervor, dass auch die trockene thermische Behandlung ein vielversprechender Weg zur Entchlorung ist, der gleichzeitig die Kosten niedrig hält.

List of contents

1 Introduction

This thesis deals with a novel approach for processing zinc and iron bearing residues, such as electric arc furnace dust, with the main target to obtain a high purity zinc oxide. In the conventional process of high purity zinc oxide production the previously metallic zinc, which has been produced in the primary process, is vaporized and then oxidized to ZnO. The investigated process allows a direct production of zinc oxide from the residue. This yields the potential of many both economical as well as ecological benefits. Zinc oxide is currently utilized by a variety of industries from rubber to cosmetics. [1]

One of the main residues that will be processable in this new process is for example steel mill dust. Contrary to the Waelz process, which is currently being used for 80 % of the recycled steel mill dust, it produces no direct CO_2 emissions [2]. By 2035, the share of the Electric Arc Furnace (EAF) in the production of steel is expected to rise to 50 % globally. Meanwhile, the overall steel market is projected to grow between 1.1 and 1.4 %, per annum to 1.87 billion tons annually with new demand mainly coming from the emerging markets. [3] Typically, per ton of steel produced via the EAF route, between 12 to 20 kg of electric arc furnace dust (EAFD) are generated. [4]

Differently than expected when reading the patent for the investigated process, zinc is not precipitated as $Zn(OH)_2$, but as a zinc hydroxide chloride (ZHC) compound, namely $Zn_5(OH)_8Cl_2 \cdot H_2O$ or tetrabasic zinc chloride (TBZC). The occurrence as TBZC was discovered during the calcination of the product, which lead to significant zinc losses, due to the evaporation of zinc chloride. This was verified in a thermal gravimetric analysis as well as in a chemical analysis. Additionally, SEM pictures showed that the structure of the material resembles the structure of TBZC. Therefore, the target of this thesis is to find ways to optimize the process in a way, that the yield of zinc oxide is increased and the product quality is improved. Other possible impurities beside chlorine include lead, manganese, magnesium as well as calcium. The market for the final zinc oxide product is dependent on its chemical as well as physical properties. The main objective of this thesis however is the selective removal of chlorine while keeping the zinc yield high. This is attempted by an initial study of different means of the dechlorination of similar materials or residues. Thermodynamic simulations are conducted to show how different parameter variations effect the process of dechlorination of TBZC. In some tentative experiments the practical feasibility of the dechlorination is investigated. The calculations are compared to and verified by further experiments. Finally, the different process routes for dechlorination are analyzed while advantages as well as disadvantages are highlighted. Additionally, an alternative route for the precipitation of zinc from the leachate is investigated. The aim of this is to prevent the formation of TBZC and to include new cleaning steps for the solution, in order to achieve a product of higher purity.

2 Product quality of zinc oxides

Zinc oxide is used across a large number of industries with a global demand of around 1.5 million tons per year. The product quality required is dependent on the application area of the oxide. The largest consumer of zinc oxide is the rubber industry, consuming about 55 % of global demand. An overview of the different industries which consume zinc oxide is given in Figure 1. [5]

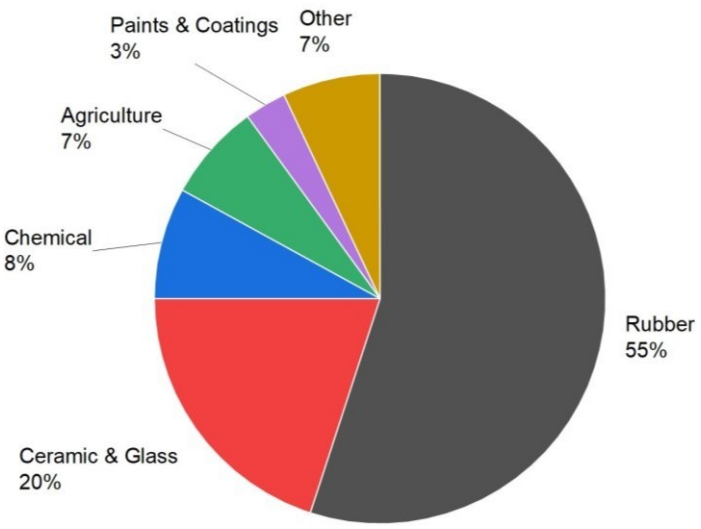

Figure 1: Share of global demand for zinc oxide by sector for the year 2015 [5]

As shown in Figure 1, the market for zinc oxide is diversified with numerous economic sectors as costumers. As a result, a lot of different qualities are needed which will be introduced in the following subchapters.

The ZnO synthesized from pure TBZC has a porous nanostructure, making it interesting for a number of applications where zinc oxide from other sources cannot be used. These applications include gas sensors or as an adsorbent for cadmium in off gas treatment. [6, 7]

2.1 Rubber industry

In the rubber industry, zinc oxide is used in the vulcanization process responsible for the majority of the global consumption of zinc oxide. The requirements set for zinc oxide in this industry sector are very strict and the testing methods are standardized by "*ASTM D4315 - 94(2006) Standard Test Methods for Rubber Compounding Material-Zinc Oxide*" or "*ISO 9298:1995 Rubber compounding ingredients -- Zinc oxide -- Test methods"* [8, 9]. Some of the relevant parameters are surface area, content of impurity elements, heat loss as well as sieve residue. [10]

According to zinc oxide supplier EverZinc, possible quality grades for use in the rubber industry are white seal, green seal and red seal zinc oxide as well as the EPM zinc oxide produced by the American Process. [11] The different quality requirements for zinc oxide in the rubber industry are summarized in Table 1.

Table 1: Example of requirements for certain qualities of zinc oxide used in the rubber industry

	Red Seal [12]	**White Seal [13]**
Appearance	White powder	White powder
Zinc oxide content (min.)	99.6 %	99.7 %
Lead content (max.)	0.2 %	0.08 %
Cadmium content (max.)	0.06 %	0.03 %
Iron content (max.)	0.02 %	0.01 %
Copper content (max.)	0.02 %	0.001 %
Manganese content (max.)	0.002 %	0.0001 %
Specific surface	4.5-6.9 m^2/g	3.5-5.5 m^2/g

Generally, becoming a supplier for a rubber producing company is very difficult and includes an up to one and a half year long testing period. [10]

2.2 Pharmaceutical industry

The requirements for chemicals in the pharmaceutical industry are very strict. The specifications of an exemplary product for the pharmaceutical industry offered my supplier EverZinc summarized in Table 2.

Table 2: Excerpt of the requirements for pharmaceutical zinc oxide

	Pharmaceutical Grade [14]
Appearance	White powder
Zinc oxide content (min.)	99.0 %
Lead content (max.)	10 ppm
Cadmium content (max.)	5 ppm
Iron content (typical)	2 ppm
Arsenic content (max.)	5 ppm
Manganese content (max.)	-
Specific surface	3.0 – 6.5 m^2/g

Only zinc oxide produced through the indirect or French process is suitable for use in this sector, due to the high requirements regarding impurities. [14] Even the quality of the intermediate product is ruled by the European Medicines Agency (EMA) in the EU or the Food and Drug Administration (FDA) in the United States. The exact requirements can be seen in pharmaceutical monograms such as the European Pharmacopoeia or the U.S. Pharmacopoeia. [10]

2.3 Glass and ceramic industry

There are no dedicated requirements for zinc oxide used in the ceramic industry. While the specifications are lower than in the rubbery industry, there can also be higher requirements for certain areas such as medical technologies or electronic components. [10] Nonetheless, zinc oxide of lower quality can be sold into the glass or ceramic sector. [15] In both glass and ceramics industry, zinc oxide is used to improve the resistance of the material towards thermal and mechanical shock [10, 16]. For example, Green Seal or EPM zinc oxide from the American process are products used in the ceramics industry. [17] For comparison, the grades 500 for ceramics and 124G for glass offered by Canadian Manufacturer ZoChemistry are shown in Table 3. [18]

Table 3: Requirements for certain qualities of zinc oxide used in the ceramics industry

	Green Seal [19]	**Grade 500 [20]**	**Grade 124G [21]**
Appearance	White powder	White powder	White powder
Zinc oxide content (min.)	99.5 %	99.9 %	99.9 %
Lead content (max.)	0.1 %	0.05 %	0.005 %
Cadmium content (max.)	0.008 %	0.01	0.005 %
Iron content (max.)	0.1 %	0.003	0.005 %
Copper content (max.)	0.02 %	0.001	0.001 %
Manganese content (max.)	0.0002 %	-	-
Specific surface	4.0 -6.0 m^2/g	4.0 -6.0 m^2/g	-

2.4 Agriculture

In agriculture, zinc oxide is utilized as fertilizer as well as a supplement to the animal feed. Both EverZinc and ZoChem recommend the same product grades for these types of application. [1, 22] The use of TBZC itself as an animal feed has also been approved by the European Union, however, the requirements concerning impurities are again very strict, as can be seen in Table 4. [23, 24]

Table 4: Requirements for zinc oxide (middle column) and TBZC (right column) used as animal feed and fertilizer

	Grade 500WSA [25]	**EU directive for TBZC [24]**
Appearance	White powder	-
Zinc oxide content (min.)	99.9 %	-
Lead content (max.)	0.05 %	30 ppm
Cadmium content (max.)	0.01 %	5 ppm
Iron content (max.)	0.003 %	-
Copper content (max.)	0.001 %	-
Manganese content (max.)	-	-
Specific surface	2.5 – 11 m^2/g	-

3 Investigated process for the production of ZnO from zinc bearing residues

In the following, the process at the center of this thesis is described. The corresponding patent has been published by Canadian researchers in 2020. The main target of the process is the hydrometallurgical extraction of zinc from different zinc-bearing residues such as EAF dust. The flow chart of the process can be seen in Figure 2. [26]

Possible raw materials for the process are different oxidic zinc-bearing ores or residues, for example electric arc furnace dust, steel mill pickle liquor or zinc dross. In the beginning (step 13), the raw material is leached with diluted hydrochloric acid. The leaching is conducted under oxidizing conditions, with the addition of an oxidant such as oxygen gas, hydrogen peroxide or nitric acid. In the next step, a solid-liquid separation is conducted with the solid residue being disposed. The filtrate is then hydrolyzed in order to recover acid and precipitate iron as well as other trivalent ions as oxides. The remaining slurry is then quenched in step 23, by diluting with water. [26]

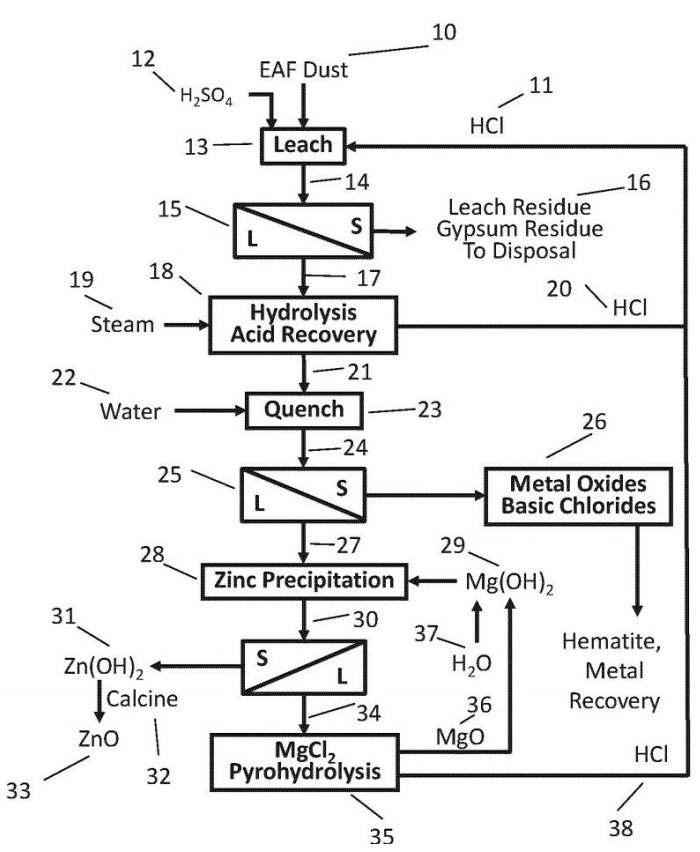

Figure 2: Concept for the treatment of zinc-bearing residues [26]

Then, the solution is once again filtrated with the solid fraction being further processed. The process route for the iron filtration cake is shown in Figure 44 in the appendix. For the following precipitation of zinc, more $Mg(OH)_2$ is added in order to raise the pH level even further to 6.0 to 8.5, preferably between 6.5 to 7.0, at a temperature of 60-65 °C. Ideally, the zinc is then precipitated as $Zn(OH)_2$ and later calcinated to ZnO. In reality, however, it has been shown that the zinc is at least partly precipitated as tetra basic zinc chloride (TBZC). The remaining $MgCl_2$ solution is processed by pyrohydrolysis in order to recover HCl and $Mg(OH)_2$ for reuse. [26]

3.1 Synthesis of the TBZC in lab scale

In order to make an investigation of a possible product upgrade for TBZC, it was first necessary to produce sufficient quantities of it by recreating the previously introduced process in a lab scale. The production of approximately 600 g TBZC requires 2.5 l of the initial solution. Instead of completely copying the process steps from the start by leaching EAF dust in lab scale, a synthetic solution was used. Figure 3 illustrates the performed treatment steps, including the labeling of obtained liquid and solid samples.

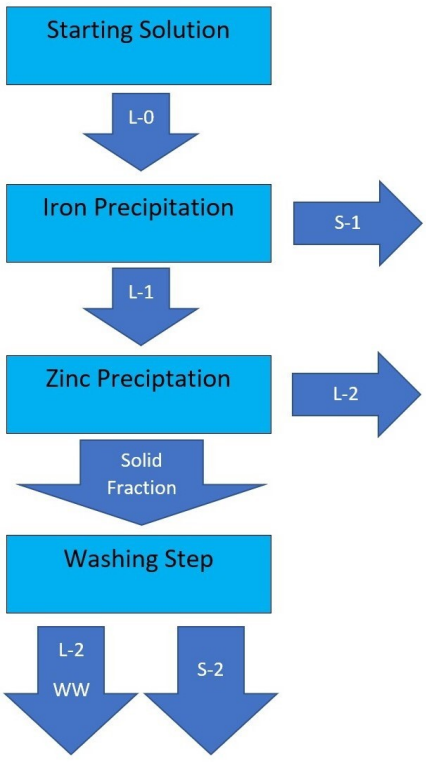

Figure 3: Flow chart for the synthetic creation of the zinc precipitate

The targeted composition of the starting solution is based on previously conducted experiments at Andritz AG, leaching of an industrial steel mill dust. It resembles the solution after hydrolysis acid recovery and subsequent quenching and can be seen as intermediate product number 24 in Figure 2.

3.1.1 Experimental setup

The experimental setup is shown in Figure 4. For the creation of the solution, a beaker of 5 l volume was utilized, while the $Mg(OH)_2$ suspension was kept in a 1 l beaker. Both vessels were put on a heating and stirring plate. The temperature in both liquids was supervised via IKA ETS-D6 thermocouple. The pH in the hydrochloric acid solution was monitored using an inoLab pH7110 pH-meter.

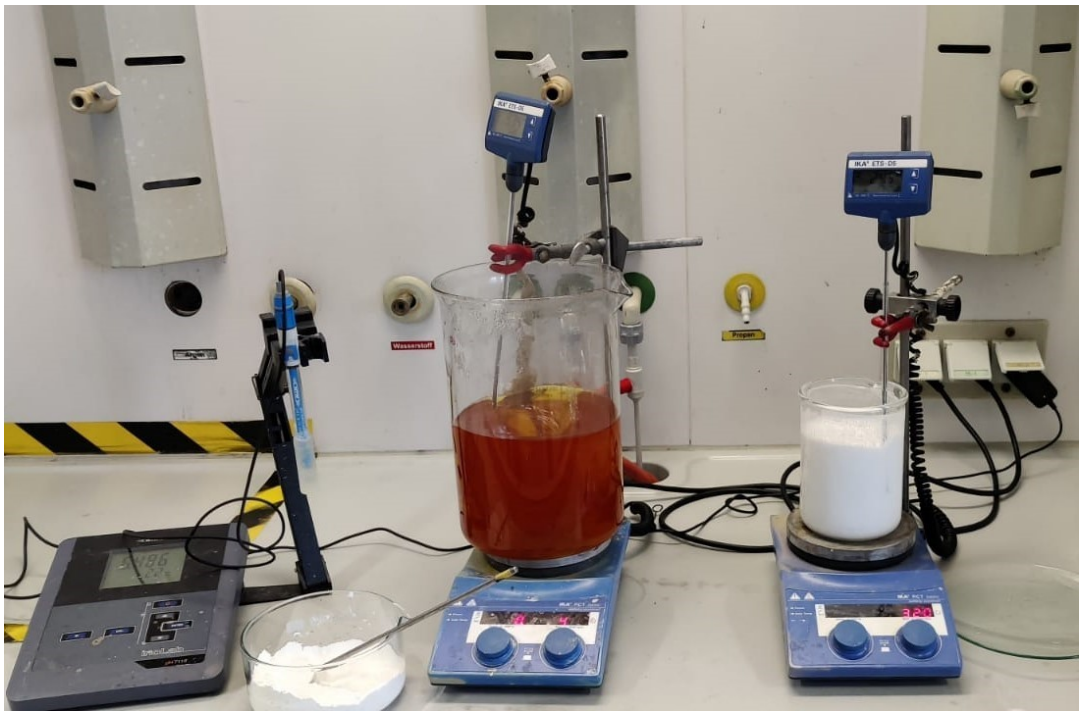

Figure 4 : Experimental setup for the reproduction of the precipitate with the hydrochloric starting solution (left) and the $Mg(OH)_2$ suspension of precipitation (right)

3.1.2 Dissolution of the metal oxides

The first step in the production of the zinc precipitate is the preparation of the synthetic starting solution. This is achieved by adding zinc oxide as well artificial impurities by dissolving metal oxides to an acidic solution. In this case, the starting point is the solution after the hydrolysis step. The target concentrations for the different elements in the synthetic solution are based on the analysis of a solution, which was generated from leaching EAF dust by the project partner. For the synthetic solution, the necessary input amount of metal oxides has been

calculated. The results can be seen in Table 5. The amount of hydrochloric acid is calculated for the stochiometric full dissolution of the metal oxides. Subsequently, water is added in order to dilute the solution, until reaching the right overall volume needed to achieve correct concentrations.

Table 5: Target concentration, as well as calculated and real input mass for the preparation of the starting solution

Element	Target concentration [g/l]	Compound	Calculated input [g]	Real input [g]
Mn	6.58	MnO	11.72	11.70
Pb	1.08	PbO	1.60	1.66
Fe	1.67	Fe_2O_3	3.30	3.39
Ca	10.74	CaO	20.72	20.78
Zn	362.50	ZnO	622.08	622.48
-	-	HCl (37 %)	1 536.41	1 543.26
-	-	H_2O	963.59	969.32

The trial is monitored by a thermocouple as well as a pH-meter. First, deionized water and hydrochloric acid are mixed in a beaker of 5 l volume. Afterwards, the metal oxides, shown in Figure 5, are added in order to reach the desired content of zinc and impurity elements.

Figure 5: Metal oxides used (PbO, Fe_2O_3, MnO, CaO f.l.t.r.)

When dissolving the oxides, it is important to start with the hardly soluble oxides such as PbO or MnO and add ZnO towards the end, to secure that enough free acid is available for full dissolution. It is also important to add the oxides slowly, as some oxides, for instance CaO, react quiet strongly with the acidic solution. During the dissolution of the oxides, the solution is continuously stirred.

3.1.3 Precipitation of iron

For pH adjustment during the iron precipitation a $Mg(OH)_2$ suspension was prepared. Preliminary experiments showed that approximately 700 ml of the suspension with a solid/liquid ration of 1/5 are needed. The calculated and the actual weight for the production of the $Mg(OH)_2$ suspension can be seen in Table 6.

Table 6: Calculated and real mass of $Mg(OH)_2$ used for the preparation of the first batch of suspension used for neutralization

Chemicals	Calculated input [g]	Real input [g]
$Mg(OH)_2$	140.00	140.85
H_2O	700.00	701.43

As soon as the solution and the suspension have reached a temperature of 60 °C, the precipitation step can be started. A small quantity of H_2O_2 is added to the solution in order to oxidize any present Fe^{2+} ions to Fe^{3+}. The starting pH after the dissolution of the metal oxides was 3.4. By the addition of magnesium hydroxide suspension, the pH level of the solution is raised to 4.3. Overall, 577.66 g of the $Mg(OH)_2$ suspension were added to the solution, which correlates with an $Mg(OH)_2$ amount of 116.00 g. After reaching the desired pH-level, the filtration is conducted. For solid/liquid separation, a filtration paper with a mesh size of 8-12 µm was used. The setup for the filtration process can be seen on the left side in Figure 6.

Figure 6: Experimental setup during the filtration of the solution (left), dried iron filtration cake (right)

It can be observed that even while the filtration is ongoing, the filtrate is taking on a white color, which is due to the precipitation of zinc compound as a result of the decreased solubility at lower temperatures. If the liquid is too cold during filtration, this can lead to zinc losses in the solid fraction. The iron filter cake is then dried at 110 °C in a drying cabinet. Meanwhile, the filtrate is further processed in the precipitation step of the zinc compound. The dried iron filter cake can be seen on the right side in Figure 6. It has an earthy consistency with some bigger pieces that can easily be crushed by hand. Furthermore, the light brown color points towards the coprecipitation of zinc.

3.1.4 Precipitation of zinc compound and washing of the product

The solution, where the zinc compound can be extracted, is sourced directly from the iron precipitation step. At first, it is reheated to 60 °C while being stirred with an agitator. Meanwhile, a new $Mg(OH)_2$ suspension is prepared, utilizing water and solid $Mg(OH)_2$. The masses of water and $Mg(OH)_2$ are summarized in Table 7. To raise the pH to a level of 5.4, the prepared suspension is used.

Table 7: Calculated and real mass of $Mg(OH)_2$ used for the preparation of the second batch of suspension used for neutralization

Chemicals	Calculated input [g]	Real input [g]
$Mg(OH)_2$	200.00	200.08
H_2O	1 000.00	998.32

In the second step of precipitation, the added mass of the $Mg(OH)_2$ suspension was 1 080.51 g. Due to a measuring error of the pH-meter, too much $Mg(OH)_2$ was added, resulting in a slightly higher pH-level of 5.48, compared to the planned 5.4. In order to prevent further rising of the pH level, about 4 ml of HCl were added.

In the subsequent filtration, a filtration paper with a mesh size of 2-3 µm was used due to the small expected grain size of the zinc precipitate compared to the iron precipitate.

Afterwards, the filtration cake is washed two times. The first washing step happens directly in the filter by rinsing with about one liter of 80 °C hot water. In the second step, the filtration cake is suspended in 600 ml of water and filtrated once again. Finally, the filtration cake is dried at 110 °C in a drying cabinet.

The dried filtration cake is shown in Figure 7. The filtration cake has a very fine and sandy consistency, with the bigger pieces again being easily crushed by hand.

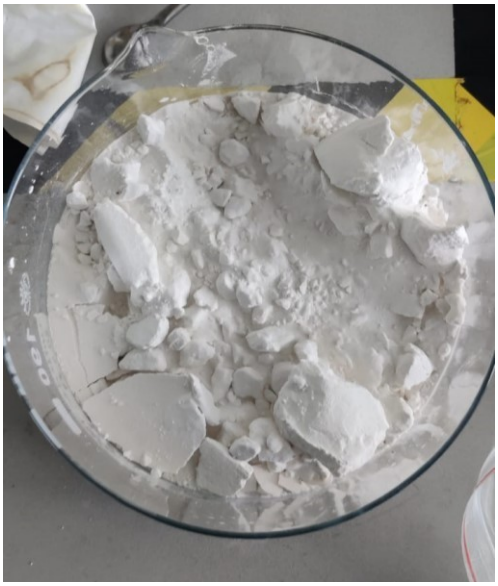

Figure 7: Washed and dried filtration cake from the precipitation of zinc compound

3.1.5 Analysis of the mass streams of the experiment and mass balance

The elemental analysis of the solution before the addition of $Mg(OH)_2$ suspension can be seen in Table 8. The value for chlorine is missing, due to a mistake made by the analyzing company where some iron that has been precipitated while shipping was dissolved again using hydrochloric acid, as a result introducing chlorine. The samples were analyzed by AMCO united assayers and samplers GmbH in Germany.

Table 8: Chemical analysis of the base solution (AMCO)

Element	Concentration [mg/l]
Ca	6 450
Fe	10 071
Mg	27
Mn	3 980
Pb	686
Zn	230 500
Cl	-

The composition of the solution after the precipitation of iron can be seen in Table 9. It appears that the iron precipitation was successful as a remaining iron concentration of under 1 mg/l was achieved.

Table 9: Chemical analysis after iron precipitation (AMCO)

Element	Filtrate [mg/l]	Precipitate [%]
Ca	4 592	0.1
Fe	<0.1	1.0
Mg	15 990	0.8
Mn	2 965	0.1
Pb	425	0.1
Zn	141 300	56.9
Cl	194 750	14.5

With a total weight of the filtration cake of 254.7 g and a zinc content of 56.9 % of the precipitate, 145 g zinc were lost during the precipitation of iron. The elemental analysis of the zinc precipitate can be seen in Table 10. The weight of the wet zinc precipitate was 691.0 g, while the weight of the dried precipitate was 413.5 g. The filtrate had a total volume of 3.5 l, which means 117 g of zinc were not being precipitated.

Table 10: Chemical analysis after zinc precipitation (AMCO)

Element	Filtrate [mg/l]	Precipitate [%]
Ca	3 378	<0.02
Fe	<0.1	<0.02
Mg	35 158	2.7
Mn	1 845	0.3
Pb	297	<0.02
Zn	33 500	56.8
Cl	131 250	12.3

The overall mass of zinc in the precipitate is 234.9 g. With an overall input of 500 g of zinc in the beginning, this brings the overall zinc yield of this experiment to 47.0%. The biggest losses occurred due to the coprecipitation of zinc in the iron precipitation step and through the filtrate during the zinc precipitation. In the following, different properties of the precipitate will be investigated to make sure that the precipitate at hand really is TBZC.

3.1.6 Characterization of the zinc precipitate

In the patented process [26], the precipitation of zinc as zinc hydroxide is expected, however, due to previously done analysis it is proven that it precipitates as TBZC instead. The composition of the synthetically produced TBZC has been analyzed by AMCO GmbH in Duisburg Germany and is listed in Table 10 (precipitate). The molar ratio between zinc and chlorine is 2.50, which is exactly equal to that of pure TBZC that consists of 2 mol chlorine and 5 mol of zinc per mole. The two detected main impurities in the TBZC are chlorine with 12.3 % and magnesium with 2.7 %. Both of these impurities were added during the process. The high content of magnesium is likely to be the result of exceeding the target pH-level during the zinc precipitation, resulting in partial coprecipitation of $Mg(OH)_2$. Chlorine is present due to the utilized solvent. Another notable impurity in the precipitation product is manganese, with a content of 0.3 %. The other impurities observed such as iron, lead and calcium were almost completely removed during the cleaning steps or remained in the process solution. Compared to the requirements for high purity zinc oxide, it can be stated that the content of lead is sufficient. In contrast, the content of manganese is above the limit for all applications except for the ceramic products, where no limit for manganese was given.

- Morphological analysis via the SEM

Figure 8 shows two SEM pictures of the precipiate at different magnifications. The investigated sample clearly displays the typical layered structure of TBZC. The morphology is characterized by layered hexagonally shaped plates with a particle size of 5-20 µm. Additionally, there are some smaller particales recognizable due to abrasion between the plates. [27–29]

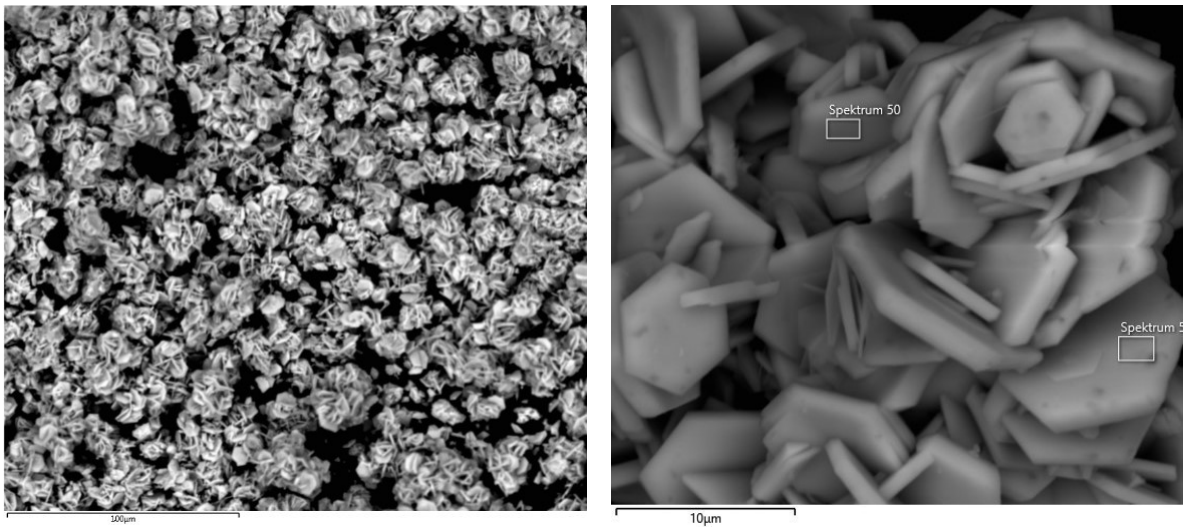

Figure 8: SEM pictures of the precipitate with lower magnification (left) and higher magnification (right)

For comparison, in Figure 9 two SEM pictures of investigated TBZC samples from literature can be seen, which exhibit the same hexagonal layered structure.

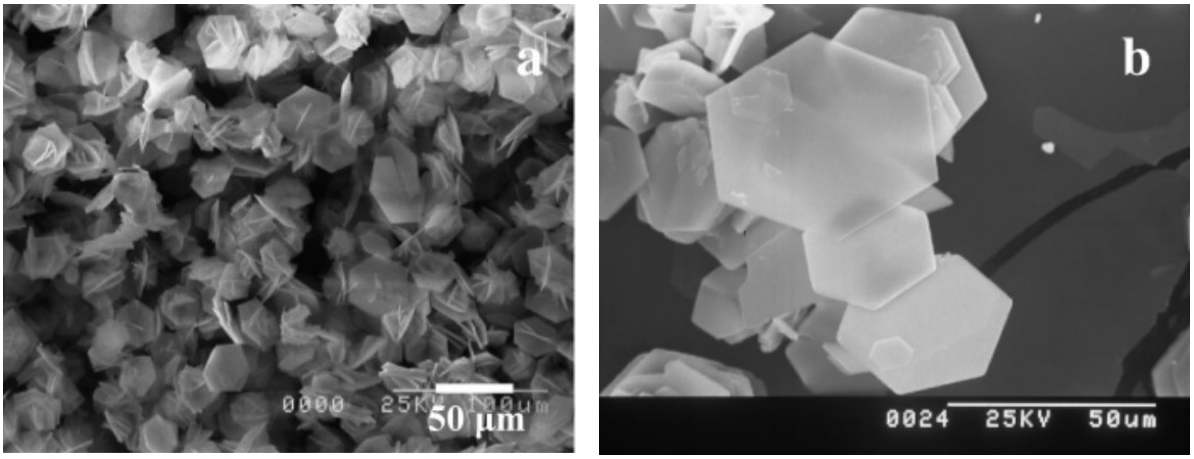

Figure 9: SEM pictures of pure TBZC from literature with lower magnification (left) and higher magnification (right) [27]

- Thermal analysis

Subsequently, a thermal analysis of the precipitate via thermogravimetry (TG) and differential thermal analysis (DTA) on an apparatus of the type Netzsch STA 409 was conducted. The heating rate was set to 10 °C/min, with a maximum temperature of 1200 °C and synthetic air as atmosphere. The result of thermal analysis of the precipitate can be seen in Figure 10. It is visible that the mass loss takes place in two steps. The first mass loss, starting at around 170 °C, resulted in a decrease in mass of 12.64 %. This can be linked to the evaporation of crystal water and the water from the calcination of zinc hydroxide. Per mole of TBZC, five moles of water are evaporated, resulting in a theoretical mass loss of 14.54 %. This is higher than the mass loss that was observed in the experiment.

The second mass loss, which ranges from 400 °C to 630 °C, can be traced to the evaporation of $ZnCl_2$ and sums up to 23.11 %. For 100 % of TBZC during the evaporation of $ZnCl_2$, a mass loss of 26.48 % is expected, which is again lower than the stochiometric amount for this step. During the whole thermal analysis, a mass loss of 41.02 % is expected, compared to an observed mass loss of 35.75 %. This can be explained by the partial hydrolysis of zinc chloride, which will further be explained in chapter 3.2.3.

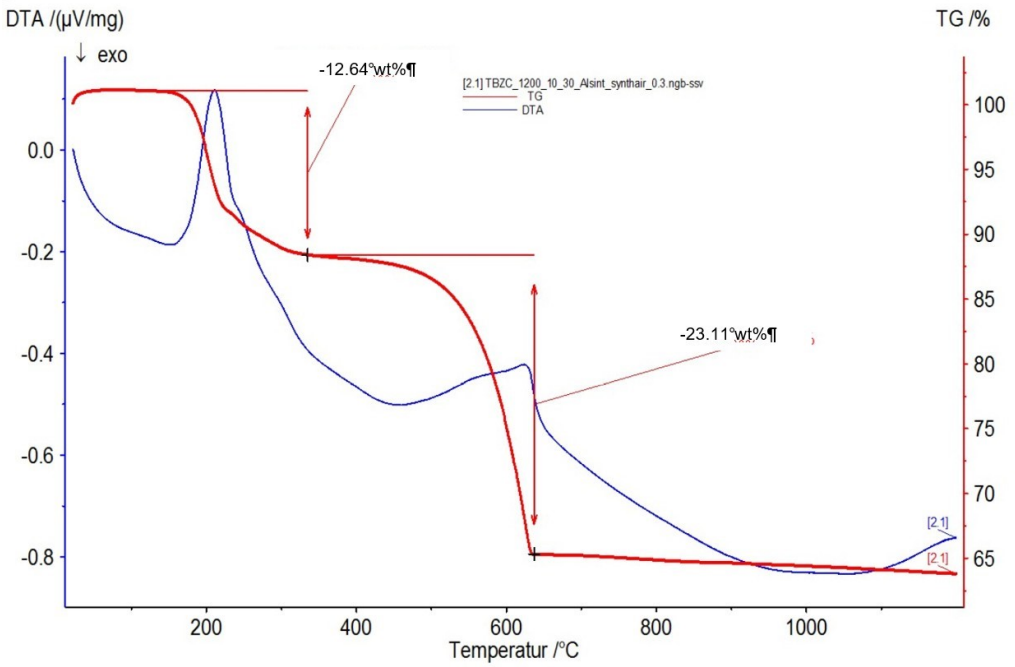

Figure 10: Analysis curve (TG/DTA) from the thermal analysis of the TBZC precipitate

The curve for the second mass loss in Figure 10 displays the typical course for the evaporation of chlorides. In the beginning at around 400 °C, a slow start is visible, which can be traced back to the slowly increasing vapor pressure of zinc chloride with rising temperatures. The abrupt stop of the mass loss at 630 °C is due to the fact that no zinc chloride remained to be evaporated beyond that temperature.

3.2 Pyrometallurgical removal of chlorine

In order to find possibilities for the dechlorination of the TBZC intermediate product, it can be beneficial to look at industrial processes dealing with the same issue. For instance, when looking at the dechlorination of EAF dust, two routes for halogen removal seem to be transferable to the dechlorination of TBZC. The first one is the clinkering process, which takes advantage of the high vapor pressure of chlorides at higher temperatures. Another benefit of the process is that other volatile impurities, such as lead and cadmium, can be removed. [10] The pyrohydrolysis, another possibility, uses thermal treatment in a steam atmosphere to first split halogen compounds to then remove the halogens as hydrochloric or hydrofluoric acid. [30]

3.2.1 Clinkering

Clinkering can be used to clean Waelz Oxide from halogens and other volatile impurities. The process is usually conducted at temperatures ranging between 900 and 1100 °C. Refining is achieved through volatilization of impurities with a high vapor pressure, which are mainly

halogens, halogenides as well as lead and cadmium oxides. To prevent the reduction of zinc oxide to zinc which also evaporates at these temperatures, it is important to ensure an oxidizing or neutral atmosphere in the furnace. [31, 32]

Coming back to the case of clinkering the investigated TBZC intermediate product, it is presumed that $ZnCl_2$ will be evaporated leading to a loss of up to 20 % of the zinc into the dust phase. [33] A possibility to counteract the loss of zinc would be the collection of the dust with subsequent soda leaching in order to remove chlorine. The zinc hydroxide or carbonate from the leaching step can then be recirculated back into the clinker step.

The thermal treatment for dechlorination of ZnO by microwave roasting has been investigated as an alternative by Chinese researchers. It is reported that chlorine extraction over 95 % has been achieved, however, there was no report of the amount of zinc lost during the treatment. [34] There have also been experiments to dechlorinate zinc dross by microwave roasting. The rate of dechlorination was measured by chromatography of the off gas. Differently to what has been expected, mainly Cl_2 and HCl were in the off gas while $ZnCl_2$ transformed to ZnO. [35] The treatment is advantageous due to different absorbance of microwaves for halide compounds and oxides, which may cause the process to be more energy efficient. Furthermore, using microwave heating minimizes off gas volume and CO_2 emissions. [35]

In industrial environments, there is always a certain amount of steam present in the air due to natural air humidity and water in the off gas of burners. As a result, even while clinkering without the further addition of steam, partial hydrolysis of $ZnCl_2$ can be anticipated.

3.2.2 Pyrohydrolysis

During pyrohydrolysis, the TBZC is treated with hot steam at 850 – 900 °C, causing the compound to split up. It is then hydrolyzed by the steam, forming HCl and ZnO. As a result, it is possible to remove up to 98 % of chlorine, while keeping the loss of zinc oxide low. This is, however, contrasted by longer process time of up to 8 h as well as a high resulting energy consumption. [30] Additionally, due to the large quantities of water vapor and the highly corrosive off-gas, a complicated exhaust gas routing is necessary. [31] The behavior of $Zn_5(OH)_8Cl_2 \cdot H_2O$ in humid atmospheres upon heating has already been investigated in multiple publications and the underlying reaction mechanisms are explained in the following chapter. [27, 33, 36, 37]

3.2.3 Behavior of TBZC during thermal treatment

There have already been multiple publications on the decomposition of $Zn_5(OH)_8Cl_2 \cdot H_2O$, however, there is still no complete consensus over the exact decomposition steps and reactions [33, 36–39]. In the following, a quick overview of different theories on the thermal

decomposition of $Zn_5(OH)_8Cl_2 \cdot H_2O$ is given. In order to make the different theories more comprehensible, a chronological approach for the presentation of different scientific publications has been chosen.

In 1967, the first report about the thermal decomposition of ZHC was published by a Spanish research group. In this report, the decomposition has been observed, using differential thermal analysis (DTA), gravimetry, x-ray diffractometry (XRD) as well as surface area analysis. Over the course of thermal experiments, three endothermic peaks were identified, two of which were ascribed to the vaporization of both the crystal and the structural water in the compound, while the third one was linked to the formation and evaporation of HCl. In this paper, the first chemical equation linked to the decomposition of $Zn_5(OH)_8Cl_2 \cdot H_2O$ was formulated, which can be seen in equation (1). [37]

$$Zn_5(OH)_8Cl_2 \cdot H_2O \rightarrow 5ZnO + 2HCl\,(g) + 4H_2O\,(g) \quad (1)$$

Following this theory, another publication which also has been released in 1967 suggests that the removal of water from the compound is happening in two stages, according to equations (2) and (3). [38–40] The split of the crystal water happens from 110 °C to 165 °C. [39] Other researchers reported that the evaporation takes place at lower temperatures around 100-110 °C. [38, 39, 41]

$$Zn_5(OH)_8Cl_2 \cdot H_2O \rightarrow Zn_5(OH)_8Cl_2 + H_2O\,(g) \quad (2)$$

$$Zn_5(OH)_8Cl_2 \rightarrow 4ZnO + ZnCl_2 + 4H_2O\,(g) \quad (3)$$

The final mass loss from 400-535 °C was described to be the evaporation of $ZnCl_2$. The difference in mass loss between the calculated full evaporation of $ZnCl_2$ and the mass loss during the experiment has been attributed to the partial hydrolysis of $ZnCl_2$ to ZnO, according to equation 4. [28, 38]

$$ZnCl_2 + H_2O \rightarrow ZnO + 2HCl \quad (4)$$

More than a decade later, another contribution on the topic was published by Rasines and Morales de Setién. In this publication, the formation of Zn(OH)Cl as an intermediate compound between 165 °C and 210 °C was suggested (eq. (5)). [39]

$$Zn_5(OH)_8Cl_2 \rightarrow 2Zn(OH)Cl + 3ZnO + 3H_2O \quad (5)$$

This compound afterwards decomposes from 210 °C to 300 °C according to equation (6), creating an endothermic peak at around 270 °C. In previous papers, this endothermic peak has been attributed to the melting of $ZnCl_2$ or the second dehydration step. [37, 39]

$$2Zn(OH)Cl \rightarrow ZnO + ZnCl_2 + H_2O \quad (6)$$

The $ZnCl_2$ formed in equation (6) later evaporates between 300 °C and 800 °C. Similar to what was reported in previous publications, the researches observed a difference between the calculated stochiometric mass loss of 41.01 % and the actual mass loss of 38.7 %, which was attributed to the partial hydrolysis of the $ZnCl_2$ formed. Another important factor brought up by this paper is that the decomposition mechanisms of $Zn_5(OH)_8Cl_2 \cdot H_2O$ do not differ between an O_2 and an N_2 atmosphere. [37, 39]

The theory of Zn(OH)Cl being formed as an intermediate compound was later suggested again by another research group. However, using high temperature powder XRD, they found out that the $Zn_5(OH)_8Cl_2 \cdot H_2O$ directly decomposed to Zn(OH)Cl and ZnO without the previous splitting the crystal water, according to equation (7). [38, 40]

$$Zn_5(OH)_8Cl_2 \cdot H_2O \rightarrow 2Zn(OH)Cl + 3ZnO + 4H_2O\ (g) \quad (7)$$

A team from the university of Madrid also investigated the influence of the heating rate on the decomposition mechanism of the $Zn_5(OH)_8Cl_2 \cdot H_2O$. Their theory is again based on the formation of the intermediate product Zn(OH)Cl, which has been found in an XRD measurement. However, unlike Rasines and Morales de Setién, they found out that the further decomposition is dependent on the heating rate. [37, 42] The first reaction step follows equation (7) while the further split of the compound is described by equation (8). According to the paper, a fraction of the $ZnCl_2$ is formed as hydrated salt, which is hydrolyzed at higher temperatures. [37, 42]

$$2Zn(OH)Cl \rightarrow ZnCl_2 \cdot xH_2O + ZnO + (1-x)\ H_2O\ (g) \quad (8)$$

The parameter x stands for the fraction of the $ZnCl_2$ which will be hydrolyzed, forming ZnO and HCl. Experiments have shown that for a heating rate of 5 °C/min x was 0.47, while a lower heating rate of 1 °C/min resulted in x approaching 1, meaning that $ZnCl_2$ was fully hydrolyzed to ZnO. It is also important to note that the dechlorination was completed at lower temperatures when using a lower heating rate. This was shown through comparison of thermal treatment

with 1 °C/min and 5 °C/min heating rates. Another interesting aspect in this publication is that in the lower heating rate experiment still air was used in comparison to an air flow in the experiment with higher heating rate. The decomposition mechanisms for $Zn_5(OH)_8Cl_2 \cdot H_2O$ according to Garcia-Martinez and Vila can be seen in Figure 11. [42]

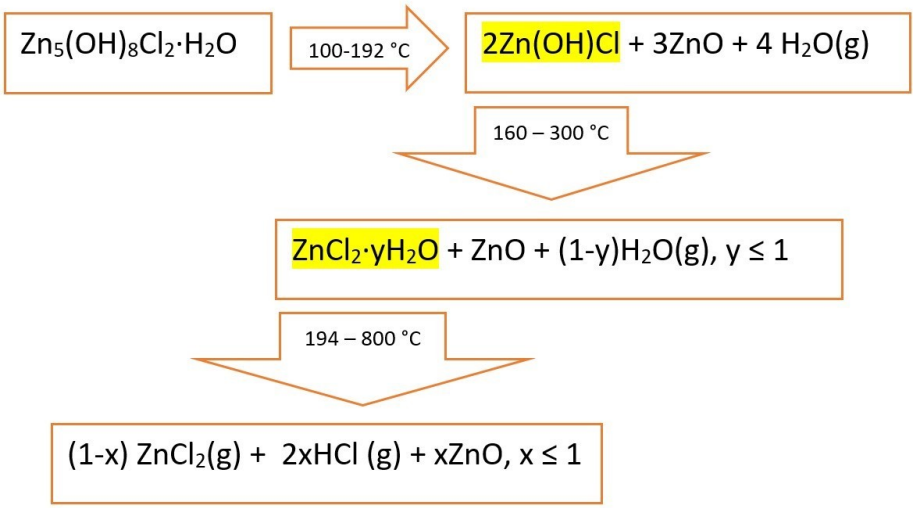

Figure 11: Visualization of decomposition mechanisms of $Zn_5(OH)_8Cl_2 \cdot H_2O$ as proposed by Garcia-Martinez [42]

In 2009, a Japanese research group has proposed another theory on the thermal decomposition of ZHC. This theory contradicts the other papers as it introduces the formation of $Zn(OH)_2$ as an intermediate product. While the first reaction happens according to equation (2), further reaction happens at around 175 °C following equation (9) and (10). [43]

$$Zn_5(OH)_8Cl_2 \rightarrow 3Zn(OH)_2 + 2\,Zn(OH)Cl \quad (9)$$

$$Zn(OH)_2 \rightarrow ZnO + H_2O \quad (10)$$

The latest paper on the topic of thermal decomposition was a review paper published by researchers of the Kiadó University Budapest, which provides an overview of the work previously done on the topic. The researchers agreed on the reaction to Zn(OH)Cl as an intermediate product from 100 °C to 192 °C, followed by the formation of $ZnCl_2$ between 160 °C and 300 °C, being the most plausible theory. This $ZnCl_2$ can be hydrated, making following hydrolysis more likely. The evaporation or hydrolysis of $ZnCl_2$ is happening subsequently between 194 °C and 800 °C. [37]

Additionally, an Australian research group has presented experimental results specifically on the topic of thermal decomposition in humid atmospheres. In order to observe the occurring reactions, the researchers conducted in situ synchrotron radiation XRD experiments. An overview of the findings is presented in Figure 12. [33]

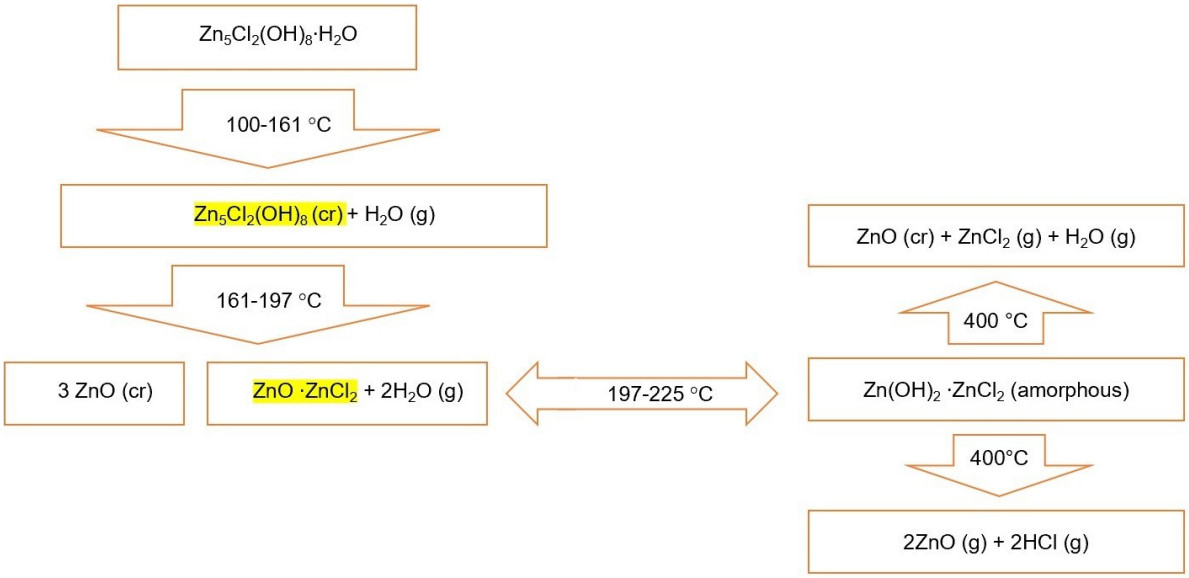

Figure 12: Visualization of mechanisms during the thermal decomposition of $Zn_5(OH)_8Cl_2 \cdot H_2O$ as proposed my Moezzi and Cortie [33]

The findings vary slightly from the results of the Spanish research group in the aspect that they suggest different intermediate compounds. While they do not confirm the occurrence of the Zn(OH)Cl compound from 160 °C to 300 °C, amorphous $Zn(OH)_2 \cdot ZnCl_2$ is formed. From this compound, the further reaction is based on whether steam is present, in order to make a hydrolysis of the $ZnCl_2$ possible. The other reaction would involve the dissociation of $Zn(OH)_2 \cdot ZnCl_2$, followed by evaporation of $ZnCl_2$. [33]

Finally, it can be said that no final consensus on the definitive decomposition mechanism of TBZC has been reached yet. However, different publications suggest that a thermal removal of chlorine without the evaporation of $ZnCl_2$ is possible. This can be achieved by using a low heating rate or a humid atmosphere. [33, 42]

3.2.4 Thermodynamic consideration

In the following subchapter, the results of thermodynamic calculations on different parameters in the thermal treatment of TBZC are presented. The calculations were made using the Factsage Equilib module. Normally, thermodynamic calculations would not be possible, as the compound $Zn_5(OH)_8Cl_2 \cdot H_2O$ is not available in the FactSage database. However, as mentioned in the previous chapter, the thermal treatment of TBZC results in the formation of intermediate products. These intermediate compounds are included in the database, making a simulation of the thermal dechlorination possible if the alternative starting compounds are used. [44]. Based on the different theories on thermal decomposition, there are three different starting mixtures which can be chosen for thermodynamic calculations. The different starting

mixtures, which replace TBZC as starting point in the calculations, are listed in Table 11. In the left column, the respective starting mixture is shown, while in the middle column number of the underlying equation is given. Lastly, the source of the chemical equation and its underlying decomposition mechanism in the literature can be seen in the right column.

Table 11: Different starting mixtures for the thermodynamic calculations

Starting mixture	Based on reactions from	Reference
$4ZnO + ZnCl_2$	(2) and (3)	[38]
$2Zn(OH)Cl + 3\ ZnO$	(7), Figure 11	[37, 42]
$4Zn(OH)_2 + ZnCl_2$	Figure 12	[33]

The results of the thermodynamic calculations for the extraction of chlorine are presented using three key figures. The first two being the “Chlorine Extraction” and “Zinc Extraction” described in equations (11) and (12).

$$Chlorine\ Extraction\ = \frac{Cl_{Gas}}{Cl_{Start}} * 100\% \tag{11}$$

$$Zinc\ Extraction\ = \frac{Zn_{Gas}}{Zn_{Start}} *\ 100\% \tag{12}$$

The third figure concerning the presentation of the results of the thermodynamic calculation is the separation factor. In case a perfect separation between zinc and chlorine is reached, where all chlorine is removed while no zinc is lost, the separation factor becomes 1. Meanwhile, if either zinc is coextracted or chlorine remains in the product, the factor becomes smaller with a minimum of 0 for no separation.

$$Separation\ Factor\ = \frac{Chlorine\ Extraction\ -\ Zinc\ Extraction}{100} \tag{13}$$

By using the “Separation Factor”, it is possible to easily compare results from different experiments just by one number. Furthermore, the results of thermodynamic calculations can simply be visualized using this factor.

- <u>Comparison of the influence of different atmospheres</u>

Now, different atmospheres for the thermal treatment of ZHC will be compared for different starting mixtures. In Figure 13, the separation factors dependent on the atmosphere for the mixture 2Zn(OH)Cl and 3ZnO are plotted over the temperature.

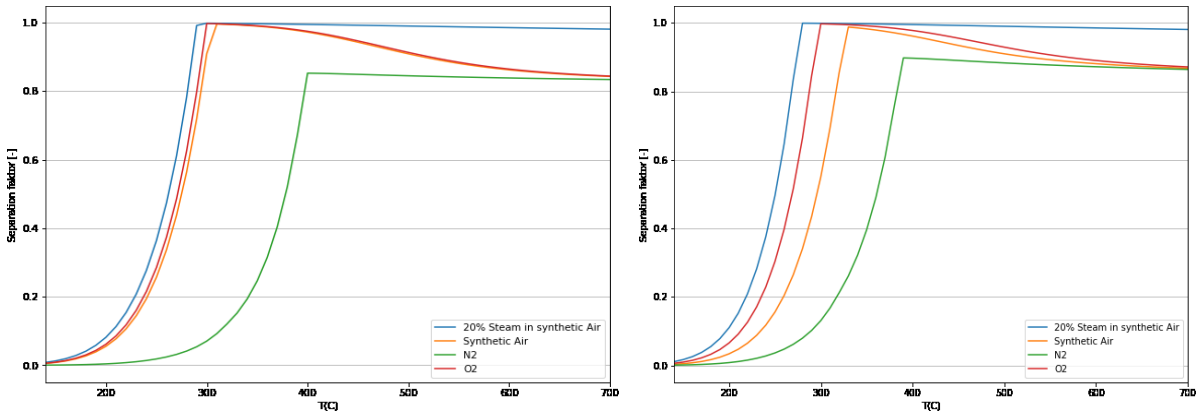

Figure 13: Comparison of separation factor for zinc and chlorine for the starting mixture 2Zn(OH)Cl + 3ZnO (left) as well as $4Zn(OH)_2 + ZnCl_2$ (right) [44]

It can be seen that the best results can be achieved with a steam atmosphere, resulting in good separation even at high temperatures. For synthetic air and pure oxygen, the results were quiet similar with the difference that the separation at higher temperatures starts to decrease again down to 0.85. Furthermore, it can be seen that in the low temperature area, pure oxygen works slightly better than synthetic air. Using a nitrogen atmosphere causes the worst results with a maximum separation factor of only 0.83.

In order to get a more in depth view, the extraction factors of zinc and chlorine are plotted over the temperature in the following figures. In Figure 14, it can be seen that for both synthetic air and steam atmosphere the extraction of chlorine reaches 100 %, starting at 300 °C. However, with rising temperatures, starting at 300 °C, zinc starts to evaporate very likely as $ZnCl_2$ into the gas phase. This effect is minimized when simulating the thermal treatment with a steam atmosphere. In Figure 14, it can also be seen that when using a nitrogen atmosphere, the extraction of zinc into the gas phase again most likely as $ZnCl_2$ is already significantly higher at lower temperatures.

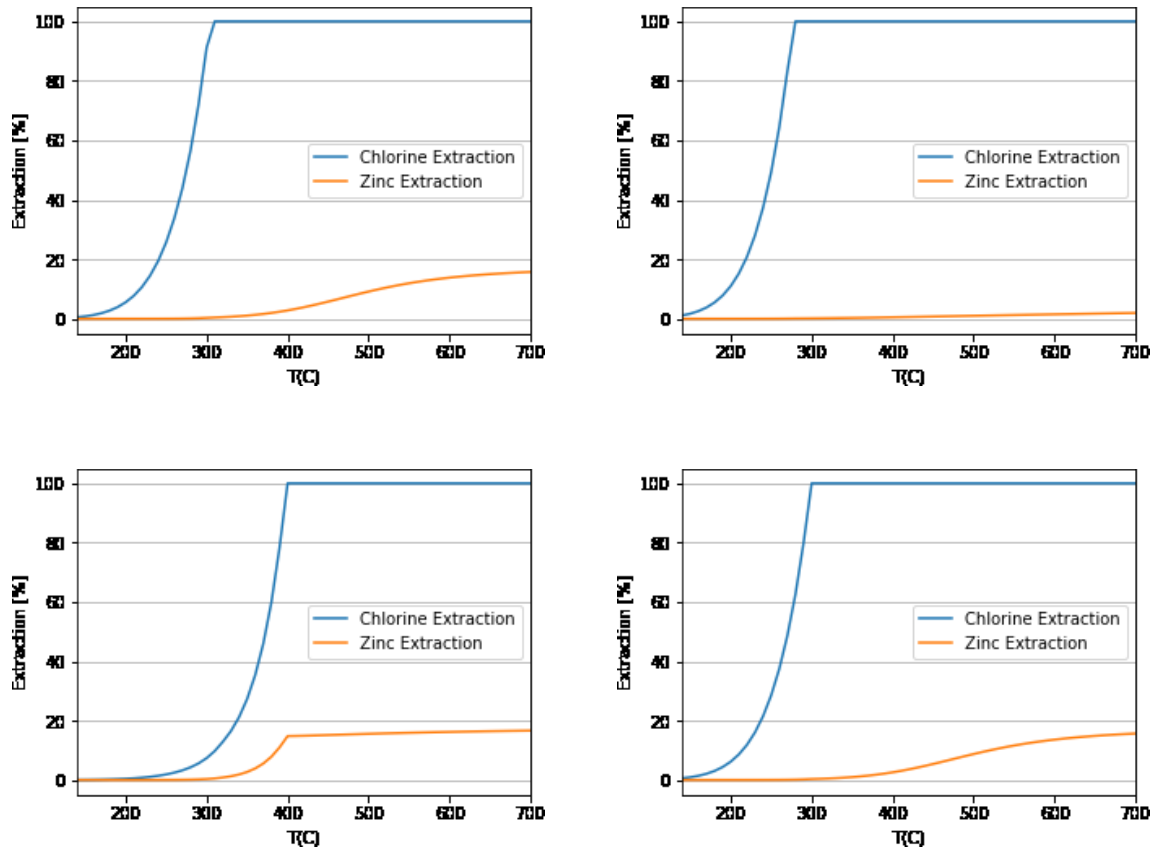

Figure 14: Comparison of the extraction of zinc and chlorine from the 2Zn(OH)Cl + 3 ZnO mixture for synthetic air (left top) air with 20 % steam (right top) N_2 (left-bottom) and O_2 (right-bottom) atmospheres [44]

- <u>Influence of the pressure on the separation</u>

The influence of the system pressure on the separation factor can be seen in Figure 15.

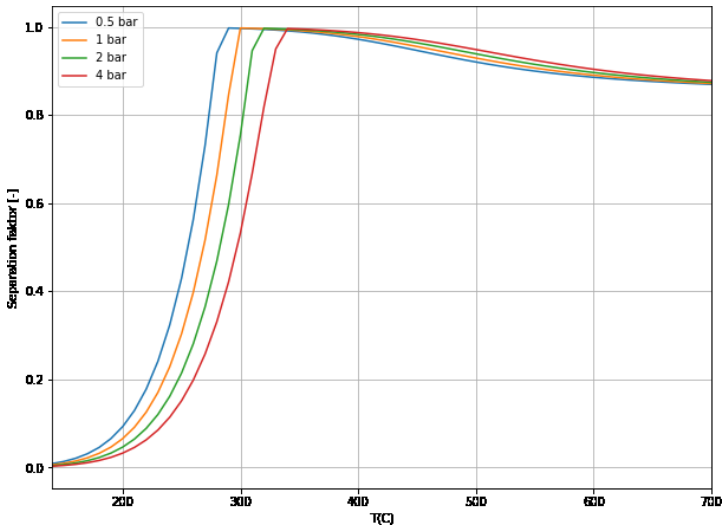

Figure 15: Comparison of the separation factor at different system pressures for the starting mixture $4Zn(OH)_2 + ZnCl_2$ under O_2 atmosphere [44]

It is noticeable that the extraction maximum shifts to higher temperatures when the pressure is raised. After reaching the maximum separation, the difference is only minimal. This is in accordance to Le Chatelier's principle, preferring the formation of a gaseous product when the pressure in the system is lowered.

- Comparison of different steam atmospheres

In the following, different steam atmospheres are compared. One important factor that is being considered is what impact a higher partial pressure of steam has on the separation of zinc and chlorine. The results can be seen in Figure 16 on the left side. Different partial pressures of steam only have a slight difference on the extraction at both low and high temperatures. From a thermodynamic view, the maximum separation factor is not influenced by the partial pressure of the steam. However, it can be noticed that with rising content of H_2O in the atmosphere, the decrease of the separation at higher temperature is lower.

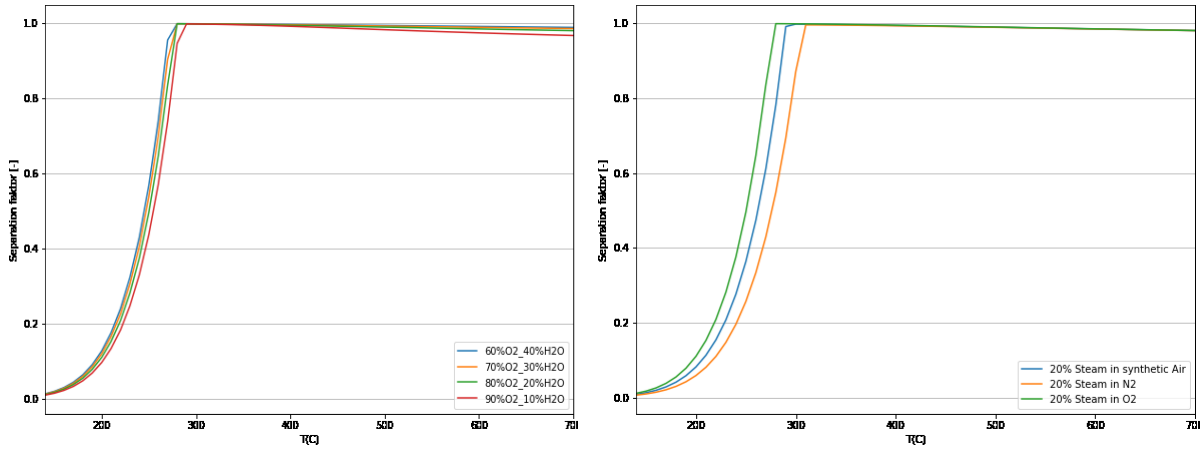

Figure 16: Comparison of the influence of different steam partial pressures (left) and different carrier gases for the steam (right) on the separation factor [44]

According to thermodynamic simulation, a variation of the carrier gas used for the steam atmosphere only has little influence on the maximum separation factor of zinc and chlorine. However, a slightly better separation can be noticed for oxygen and synthetic air at lower temperatures.

- Impact of the starting compound on the extraction

As mentioned at the start of the chapter, as TBZC is not included in the FactSage database it needs to be replaced by different compounds. The three mixtures are based on the different theories of decomposition of TBZC under thermal treatment. In Figure 17, these different

starting mixtures are compared, showing that results vary only slightly based on the reactants for an oxygen atmosphere.

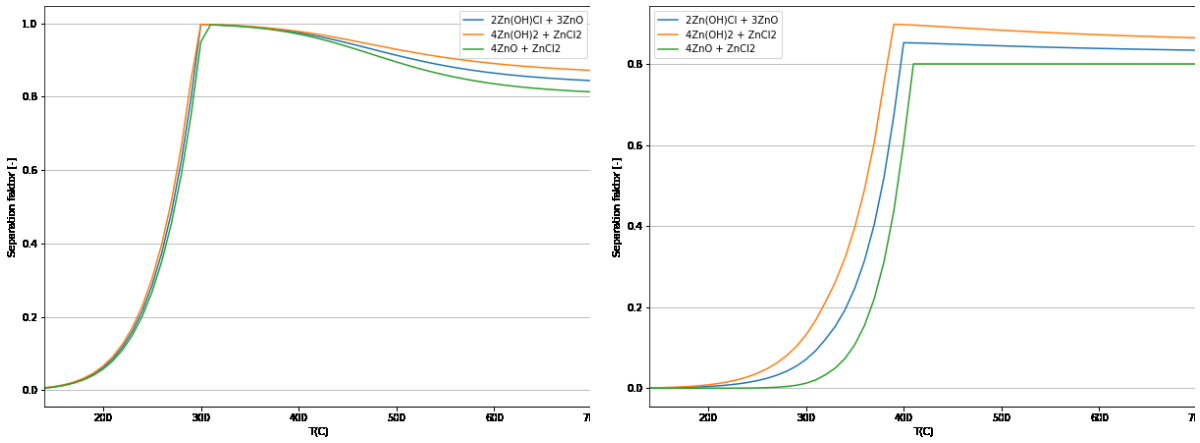

Figure 17: : Comparison of the impact of different mixtures on the extraction in O_2 atmosphere (left) and N_2 atmosphere (right) [44]

The difference between the various starting compounds can only be seen at higher temperatures when the separation factor starts to decrease again. For nitrogen, much bigger differences between the different simulations can be noticed as the maximum extraction varies based on the reactants. A possible explanation for this is the different amount of water built into the different compounds, which make the hydrolysis of $ZnCl_2$ possible and oxidizes the zinc as a result. While 4ZnO and $ZnCl_2$ (green curve) have no water that can be released at higher temperatures, four mol of water are produced during the thermal decomposition of $4Zn(OH)_2 + 2\ ZnCl_2$ (orange curve). The water can then further react with $ZnCl_2$, hydrolyzing it.

3.2.5 Thermogravimetric experiments

As already mentioned, clinkering as well as pyrohydrolysis are two possibilities for the removal of chlorine from the zinc precipitate. After thermodynamic calculations, the possibilities of thermal treatment of the product are further investigated in thermogravimetric experiments.
A Netzsch STA 449 F3 was used for these experiments. Additionally, auxiliary devices for the heating of the scale, the creation of the steam atmosphere, etc. were utilized. For the transfer of the steam from the vapor generator to the STA ,a heated tube with a temperature of 180 °C was used to prevent condensation. In order to make a comparison between the experiments possible, the heated tube was also turned on during experiments where no steam was used. The experiment was conducted using a heating rate of 5 °C/min with N_2 as protective gas for the scale. The flow in protective gas was 15 ml/min while the flow of the reaction gas was 0.8 l/min. In order to ensure that the atmosphere is saturated with water steam before further heating, an isothermal interval at 140 °C has been added before further heating to 800 °C. The

maximum temperature of 800 °C has been chosen, to guarantee the removal of chlorine from the sample. The experimental setup for the thermal treatments can be seen in Figure 18. The experiment was conducted in three different atmospheres: Synthetic air, steam with nitrogen as a carrier gas as well as synthetic air as carrier gas for the steam.

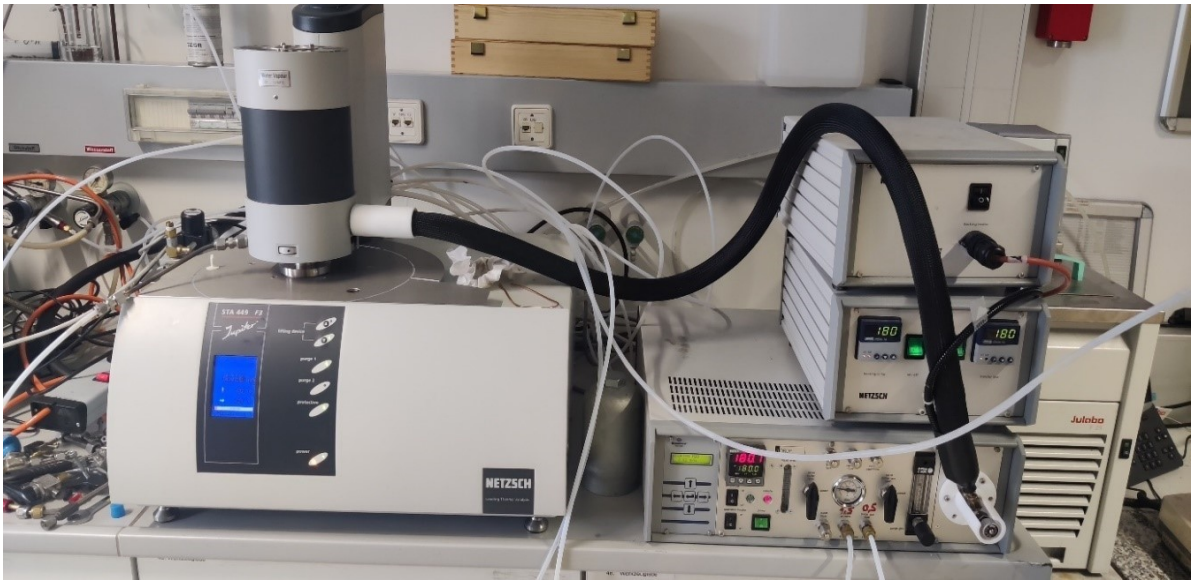

Figure 18: Experimental setup of the thermogravimetric experiments

The mass loss observed during thermal treatment is based on the reaction mechanism during the thermal decomposition of TBZC. While mass loss caused by the evaporation of water can always be observed, the determining factor is whether the $ZnCl_2$ that is formed during the evaporation is hydrolyzed according to equation (4) or evaporates into the gas phase. In case of full hydrolysis of $ZnCl_2$, water evaporates from the TBZC and chlorine is extracted as HCl, leaving five moles of ZnO in the end. In contrast, for the full evaporation of $ZnCl_2$ the one mole of zinc from the TBZC is also included in the mass loss and therefore only 4 moles of ZnO remain.

$$Minimum\ mass\ loss\ = 1 - \frac{5\ *\ M(ZnO)}{M(Zn_5(OH)_8Cl_2 \cdot H_2O} = 26{,}27\ \% \tag{14}$$

$$Maximum\ mass\ loss\ = 1 - \frac{4\ *\ M(ZnO)}{M(Zn_5(OH)_8Cl_2 \cdot H_2O} = 41{,}02\ \% \tag{15}$$

Based on these two reactions, a minimum mass loss of 26.27 % and a maximum mass loss of 41.02 % are possible for the assumption of pure TBZC. Additionally, partial hydrolysis is also possible, resulting in values between the two extremes. [37]

3.2.6 Results of thermal treatment

The results of the experiment are shown in Figure 19. It can be seen that the curves where a steam atmosphere has been used, only differ slightly based on carrier gas. The final mass loss is 28.5 % for nitrogen and 28.7 % when using synthetic air as a carrier gas. This is in line with the earlier thermodynamic calculation, where it has been shown that the carrier gas only has a minor influence on the extraction of zinc. The total extraction in the experiments with water vapor is very close to the theoretical minimum of 26.3 %. As mentioned before, this is due to the partial hydrolysis of zinc chloride and the subsequent formation of $ZnCl_2$

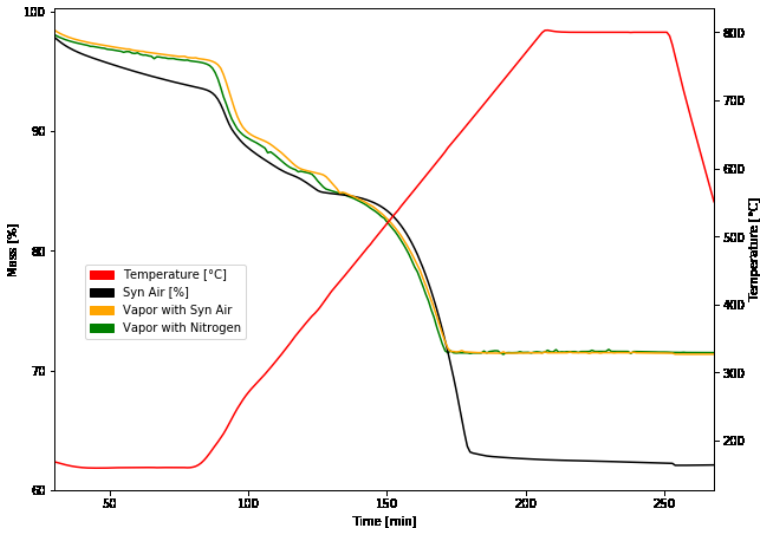

Figure 19: Comparison of the three TG curves obtained during thermal treatment of TBZC

When using dry synthetic air as atmosphere during the thermal treatment, it can be noticed that the mass loss is significantly higher compared to using a steam atmosphere. The final mass loss in this experiment was 37.9 %, which is still lower than the earlier calculated maximum mass loss of 41.0 %. Furthermore, it can be seen that the maximum mass loss was reached at around 650 °C for all three experiments, therefore no further heating is required in future experiments. It can also be expected that the dechlorination is finished at even lower temperatures when using lower heating rates. [42]

3.2.7 Analysis of the obtained product after the thermal treatment of TBZC

The chemical composition of the precipitation product is shown in Table 12. Due to the small sample quantities of about 2 g, a wet chemical analysis of the output was not possible. In order to get an overview of the effectiveness of the treatment, the material was analyzed through energy dispersive X-ray spectroscopy (EDX). Generally, the removal of chlorine through volatilization was successful. Some extraction of lead in the two experiments with steam was noticed, while the lead content did not change in the first experiment using just dry air.

Table 12: Chemical composition of the products of the thermal treatment of TBZC

	Input [%] (AMCO)	Output syn Air [%] (EDX)	Output Steam in N_2 [%] (EDX)	Output Steam in O_2 [%] (EDX)
Ca	0.0	0.0	0.0	0.00
Fe	0.0	0.1	0.0	0.1
Mg	2.7	4.4	1.8	2.5
Mn	0.3	0.4	0.4	0.4
Pb	0.0	0.1	0.0	0.0
Zn	56.8	78.7	83.0	81.9
Cl	12.3	0.1	0.1	0.1
Mass	100	62.1	72.3	76.1

An aspect that occurred during thermal treatment is the fact that the precipitation product changed its color. In Figure 20 the change in color based on the different atmospheres during treatment is shown.

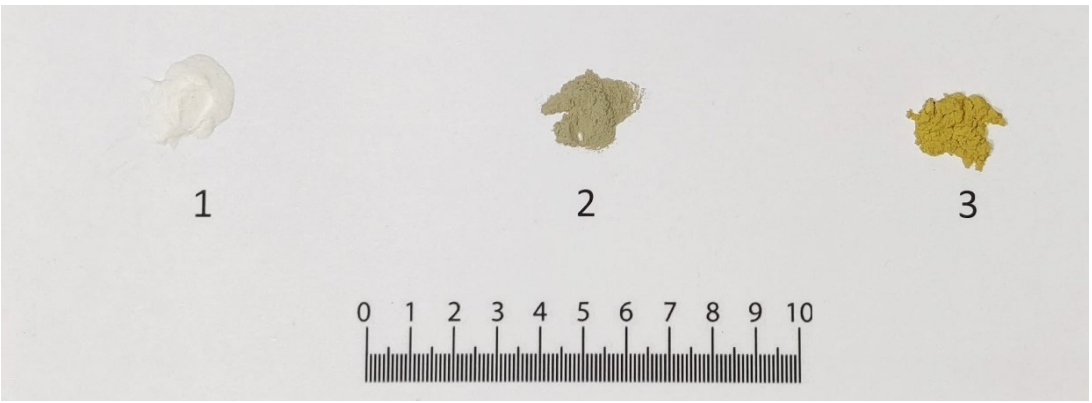

Figure 20: Color after thermal treatment compared to original sample (1) of the sample after dry thermal treatment in synthetic air (2) and in a wet N_2 atmosphere (3)

To the left, white zinc precipitate from before the thermal treatment can be seen. The sample in the middle has turned green-grey due to the thermal treatment. This color change has been observed in both experiments where oxygen was present, which were the dry experiment and the experiment where synthetic air was used as a carrier gas for the steam. The sample to the right has been treated with nitrogen gas as a carrier for the steam. As discussed in chapter 2, the appearance of the ZnO product as white powder is a main quality parameter for most applications. This is especially true for the ceramics industry, which is a good market for otherwise impure zinc oxides [15, 17]. Since the change in color for ZnO when being heated is relevant for both the thermal treatment as well as the calcination after hydrometallurgical treatment, this issue will be addressed later.

3.2.8 Interpretation of the results of thermal treatment

Similar to what has been shown in the thermodynamic calculations, the removal of chlorine at higher temperatures can easily be achieved due to its volatility. In order to compare the results of the thermogravimetric experiments, both the extraction factors and the separation factor for zinc and chlorine according to equations (11) to (13) have been calculated in Table 13.
When comparing the results in Table 13 to the results of the thermodynamic calculations in Figure 13, Figure 14 as well as Figure 16, it can be seen that for the experiment in dry air the zinc extraction was higher than calculated and therefore the separation factor was lower than expected. When looking at the zinc yield for both the experiments in humid atmosphere, it can be noticed that it is above 100 %, which is not plausible. However, this can be attributed to the measuring inaccuracy of the EDX, which cannot be completely be avoided when analyzing small samples. Nonetheless, it can be said that almost no zinc losses happened.

Table 13: Extraction of chlorine and zinc for the thermogravimetric experiments

	Syn. air	**Steam in N_2**	**Steam in syn. air**
Chlorine extraction [%]	99.3	99.2	99.6
Zinc yield [%]	86.1	104.4	102.9
Separation factor [-]	0.85	0.99	0.99

While the results when using water vapor were successful, the hydrolysis of zinc chloride when using dry air was not as satisfactory. The difference between simulation and experiment can be explained by the fact that in the thermodynamic simulations the products that are stable are calculated for equilibrium. If, however, equilibrium is not reached, the results will differ from the calculations. A cause for this may be that the heating rate was too high, causing the reaction not reach its equilibrium. This is relevant for the hydrolysis step of $ZnCl_2$, where heating too fast can cause the non-hydrolyzed $ZnCl_2$ to evaporate. While the hydrolysis seemed to take place when utilizing water vapor, the results show a different picture when using dry air. When using dry air, the water bound in the ZHC compound is used for hydrolysis after the several decomposition steps. [42]
Through optimization of the thermal treatment, it might be possible to further increase zinc yields for dry thermal treatment compared to the tentative trials. An important factor on the path of decomposition suggested by the literature is the heating rate during treatment. There, it is also mentioned that it is possible to have no zinc losses during thermal decomposition with the right parameters. [42] An important motivation to try to improve zinc yields for the dry thermal treatment is that the complexity of the industrial apparatus and therefore the investment cost is significantly lower when no steam is needed during the process. [31]

3.3 Hydrometallurgical removal of chlorine

Another possibility for the removal of chlorine is the hydrometallurgical route, namely soda leaching. The advantage of the hydrometallurgical treatment is that zinc losses become far more unlikely, as any free zinc ions normally are directly precipitated. While this treatment is already successfully being used for the dechlorination of steel mill dust, further investigation is needed to determine whether it can be applied the intermediate product at hand.

3.3.1 Soda leaching

During this hydrometallurgical process, the impure zinc oxide is industrially leached between 60 °C and 80 °C with the addition of Na_2CO_3 [31]. While leaching, halogenides and alkalis such as $ZnCl_2$ dissolve into the solution. Subsequently, the Zn^{2+} ions are precipitated as carbonate while both sodium and chlorine remain in the solution. The reaction happens according to equation (1). [30, 31, 45–48]

$$ZnCl_2 + Na_2CO_3 \rightarrow ZnCO_3 + 2NaCl \quad (1)$$

After the precipitation, a solid-liquid separation is conducted. The solid fraction is then washed again with purified water in order to remove any adherent washing solution that contains chlorine. The solution is once again filtered and the filtrate can be discharged into the sewage after the separation of heavy metals. Another possibility for treatment of the waste water is the crystallization of the salts from the solution. The condensate is then being redirected into the washing step. In order to improve the removal of chlorine, it is also possible to repeat the first leaching step as it is done in the treatment of Waelz Oxide. The extracted $ZnCO_3$ can then be calcinated to ZnO under the formation of CO_2. [10, 31]

This process is primarily used after the Waelz process in order to remove chlorine and fluorine compounds. The removal of those impurities is required for further processing of the Waelz Oxide in primary zinc metallurgy. There, contaminations with these two elements cause problems in the electrolysis. [35, 45, 49–51]. However, there has also been some research on applying this process to different residues. For instance, the process is used in the hydrometallurgical processing of copper dusts [31]. Furthermore, the removal of chlorides from zinc ash or zinc dross has been investigated in laboratory scale [50, 51].

While the results cannot be directly compared to the precipitation product investigated in this thesis, it has been shown that in the case of zinc ash, soda washing was not sufficient for chlorine removal. This is due to insoluble zinc compounds which contained chlorine. [50] These insoluble zinc hydroxide chloride compounds can also be found in the TBZC precipitation

product. A major factor in the success of hydrometallurgical treatment of the product will be whether these compounds can be dissolved, making a removal of chlorine possible.

3.3.2 Thermodynamic considerations for soda leaching

In the following, thermodynamic calculations for hydrometallurgical treatment of TBZC are discussed. As mentioned before, the compound $Zn_5(OH)_8Cl_2 \cdot H_2O$ has not been implemented in the FactSage database, which is why a different software will be used [44]. For the thermodynamic simulation the programs Hydra and Medusa were used for calculations and plotting. Both of these programs are owned by the Institute of Chemistry of KTH Stockholm [52]. An important factor to consider is that all of these calculations investigate the behavior of the solution at a temperature of 25 °C. This means that the behavior at higher temperatures, similar to the industrial soda leaching process, cannot be simulated.

A crucial aspect in the success of the hydrometallurgical dechlorination of the precipitation product is the dissolution of $Zn_5(OH)_8Cl_2 \cdot H_2O$, which would make removal of chlorine possible. In Figure 21, the zinc containing products formed from 1 mol of TBZC based on the pH-level can be seen. In this diagram, the behavior of TBZC in aqueous solution is investigated without addition of soda.

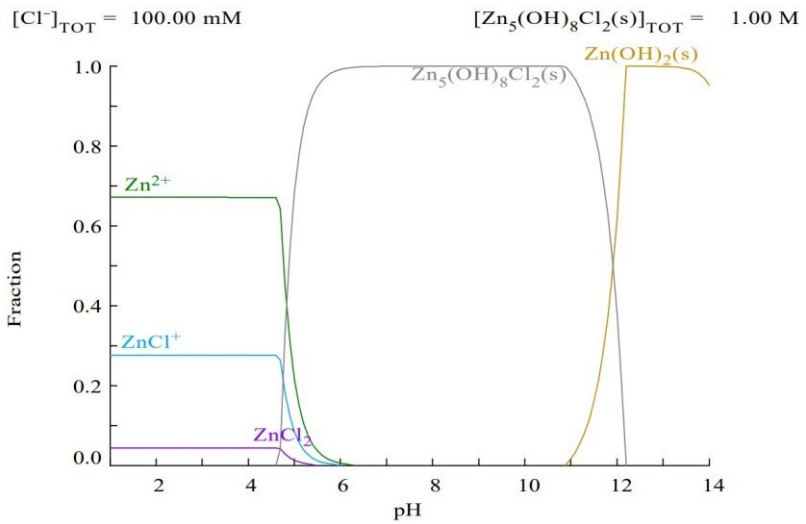

Figure 21: Fraction of zinc compounds and Ions based on different pH-levels [53]

At a pH level of around 5, solid TBZC is formed in the solution. This is in line with the pH level of 5.4, where the precipitation of TBZC was observed in the synthetic reproduction of the process described in chapter 3.1.4. It can also be observed that at pH levels higher than 12, $Zn(OH)_2$ starts to be more stable than TBZC.

In Figure 22, the stable compounds and ions in the solution are calculated as a function of the pH value after the addition of soda. At lower pH-levels, the diagram is similar to Figure 21 and

it is visible that the carbonate ions in the solution start to react with the $Zn(OH)_8Cl_2$ under the formation of $Zn(OH)_8(CO_3)_2$. It can be seen that the fraction of $Zn(OH)_6(CO_3)_2$ increases when the concentration of carbonate ions in the solution is increased. According to the thermodynamic data, all of the available carbonate ions react with the TBZC. This compound was not found in literature on the topic of soda leaching zinc hydroxy chlorides. [2, 48, 50, 54]

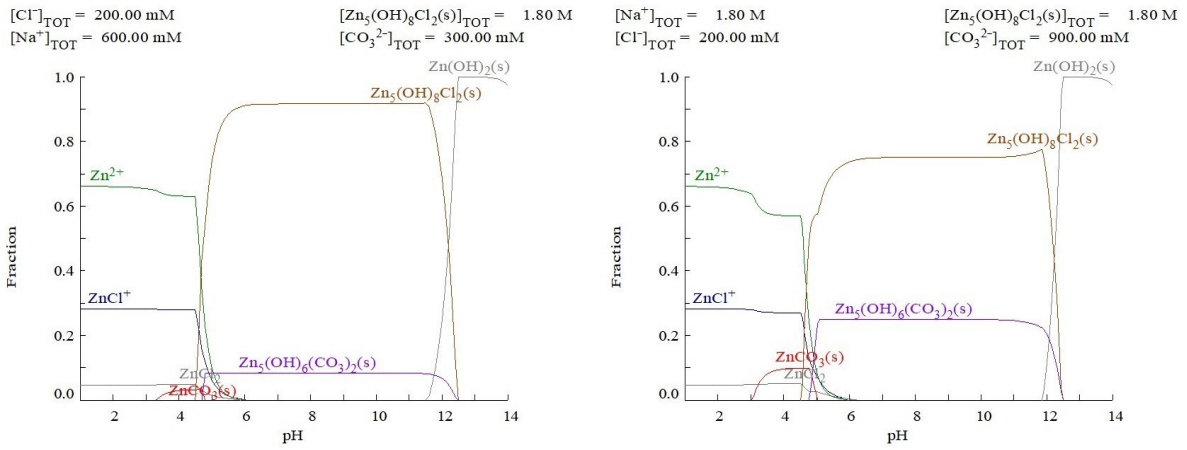

Figure 22: Stability of different compounds and ions for 0.3 mol/l (left) and 0.9 mol/l (right) of carbonate ions as a function of the pH-level [53]

In Figure 23, it can be seen that it is thermodynamically possible to convert 100 % of the TBZC to $Zn(OH)_6(CO_3)_2$ if enough carbonate ions are present. This compound can then be calcinated to ZnO at around 250 °C without any losses of zinc. Additional calculations for different carbonate ion concentrations are shown in the appendix. [55, 56]

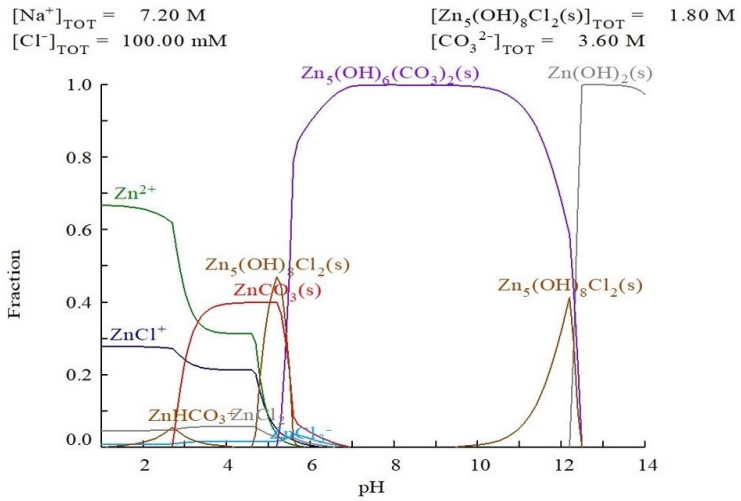

Figure 23: Stability of different compounds and ions for 3.6 mol/l of carbonate ions as a function of the pH-level [53]

The removal of chlorine from the compound without dissolution is in contradiction to the findings of researchers from the University of Istanbul, who reported that soda leaching was not possible for poorly soluble zinc hydroxide compounds. [50] Furthermore, it can be noted that a full dechlorination under the formation of $Zn_5(OH)_6(CO_3)_2$ stoichiometrically requires two mol carbonate per five mol zinc. Compared to the reaction for typical soda leaching, where for each mol of zinc a mol $ZnCO_3$ is formed, this is more efficient regarding soda consumption.
In Figure 24, the result of the addition of different quantities of soda, namely 0.9 mol/l Na_2CO_3 (left) and 1,6 mol/l Na_2CO_3 (right), is shown. As a starting reactant in this calculation Zn^{2+} ions have been used, making the underlying assumption that the TBZC compound has already been dissolved. It can be seen that between pH 4 and pH 10, depending on the concentration of carbonate, either $ZnCO_3$ or $Zn(OH)_8(CO_3)_2$ are thermodynamically stable. Lower concentrations of carbonate favor the later compound. Again, the formation of $ZnCO_3$ is undesirable, as 100 % of the zinc in the solution would be precipitated as zinc carbonate resulting in significant consumption of sodium carbonate. Another consequence would be an increase in the amount of CO_2 produced during calcination. Additional diagrams for other concentrations of carbonate ions can be found in the appendix.

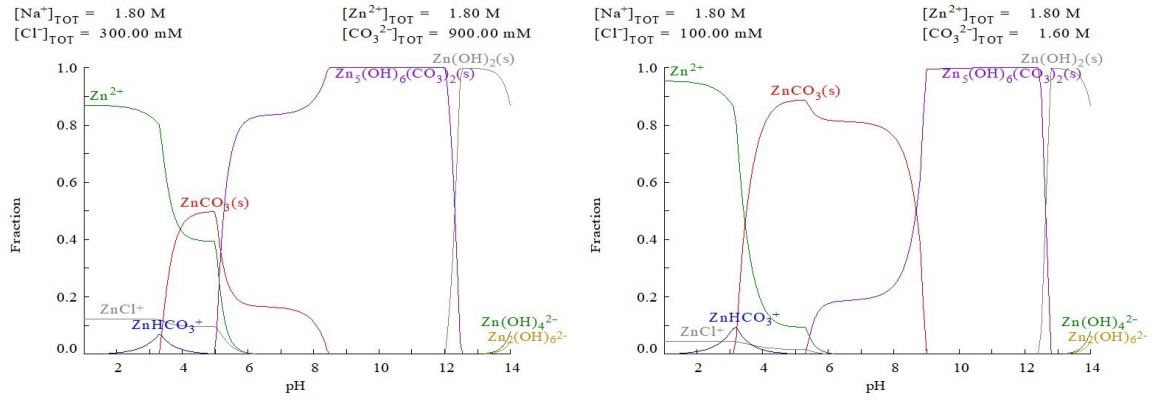

Figure 24: Comparison of different concentrations (0.9 mol/l left and 1.6 mol/l right) of carbonate ions on the stability of different compounds and ions [53]

3.3.3 Soda leaching experiments

In the following, experiments investigating the hydrometallurgical treatment of TBZC by soda leaching are described. The temperatures used in the experiments were 30 °C, 60 °C as well as 80 °C.

- Experimental procedure

The experimental setup can be seen in Figure 25. In the beginning, a suspension with a solid liquid ration of 1/5 was produced by adding 60 g of TBZC to 300 ml of distilled water.

Subsequently, the suspension was heated to the targeted temperature. After reaching the targeted temperature, the experiment lasted 120 min, while stirring and observing of the pH-level over the whole duration.

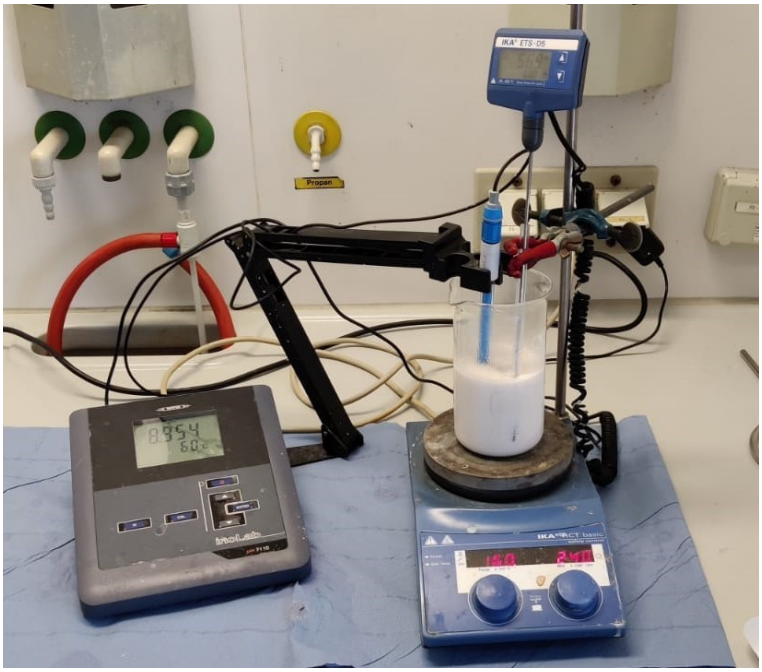

Figure 25: Experimental setup for the Soda leaching experiments on the example of the 60 °C experiment

The addition of soda was controlled based on the pH-level, which had a target value of 10. This was decided, since it was unclear how much of the chlorine in the zinc hydroxide chloride compound would actually be available for reaction. The dependance of the reaction on the temperature was very well noticeable when comparing the experiments. During the experiment at 30 °C, the pH level barely moved after reaching the target pH of 10 upon the initial addition of soda. Meanwhile at 80 °C, a falling pH level was noticed, requiring more soda as time went on. In the 60 °C as well as in the 80 °C experiments it appeared as if there were sticking points for the pH level, where the addition of large quantities of soda only had a minor impact on the pH level. However, the exact cause of this is still to be determined.
After the experiment was finished, the suspension was filtrated and the cake was rinsed with water. In the following additional washing step, the filtration cake was suspended in water and heated to 40 °C and stirred for another 45 min. Then, the slurry was filtrated once again, with the filter cake being put into a drying cabinet at 110 °C.

- Results

The results of the soda leaching experiments are summarized in Table 14. The amount of soda for controlling the pH level varied across the different experiments. It can be seen that the

amount of soda consumed was higher with rising temperature. This can be the result of a bigger fraction of the zinc in the compound being available for reaction, due to a higher degree of dissolution at higher temperature.

Table 14: Analysis of the output of the soda leaching experiments (AMCO)

Detail	Input	30 °C	60 °C	80 °C
Zn [%]	56.8	57.0	61.6	61.6
Cl [%]	12.3	12.1	8.1	0.2
Na [%]	-	<0.02	0.1	0.8
Mass [g]	60.0	58.3	56.2	55.7
Soda input [g]	-	4.0	10.2	18.6

In Figure 26, a SEM picture of soda leached precipitate can be seen. It is visible that the previously described hexagonally layered structure of untreated TBZC was destroyed. Small agglomerates of needle shaped crystals have replaced that structure. However, the overall particle size did not change.

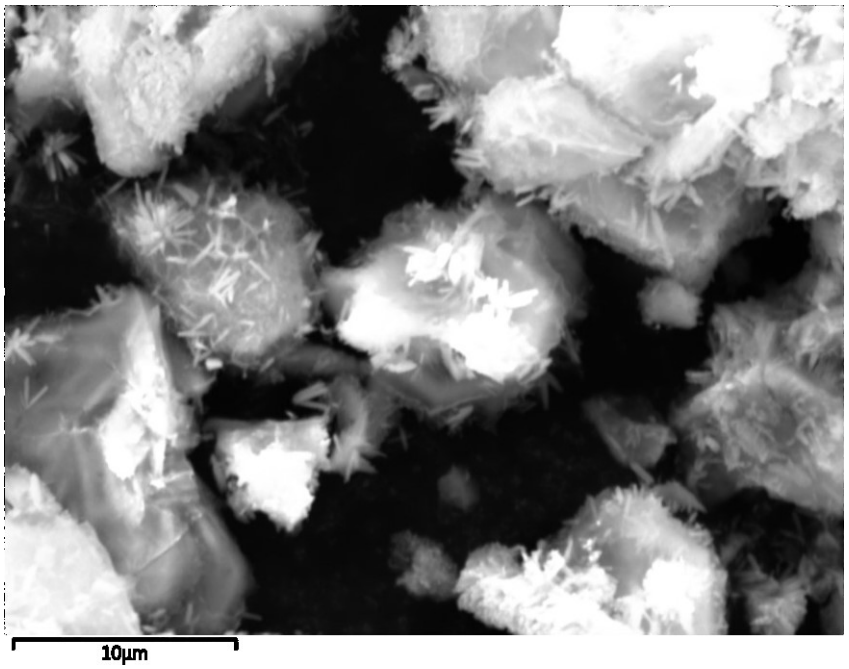

Figure 26: SEM picture of the product of the 80 °C soda leaching experiment

3.3.4 Soda leaching in the autoclave

In the previous experiments it has been shown that the removal of chlorine from the precipitation product increases with the temperature. To reach an even higher temperature

of 125 °C, the aqueous solution was put in a pressurized vessel. The pressure applied was 5 bar. Due to the higher temperature and therefore faster reaction speed, the duration of the experiment was shortened to 90 min.

- Experimental setup

Similar to the earlier conducted soda leaching experiments, the solid liquid ratio was 1/5. Because of the bigger reaction vessel in the autoclave, more suspension was required in order for the stirrer to be fully submerged. Both, the measurement of the pH-level and the continuous addition of soda are not possible in the autoclave. Consequently, the pH-level was set and the 1.3-fold stoichiometric amount of soda was added before charging the slurry into the autoclave. Therefore, 100 g of TBZC and 500 g of distilled water were used in the creation of the suspension. Before charging into the autoclave, the suspension was heated to 80 °C and 26.18 g of soda were added. After the addition of Na_2CO_3, the measured pH level was 9.19. Subsequently, the suspension was transferred to the autoclave and the autoclave was sealed.

In this experiment a autoclave of the type “polyclave” by Büchi Glas Uster with an implemented electrical stirrer was used. The temperature autoclave was controlled through a LAUDA thermostat which was connected to the autoclave through an oil circuit. The experimental setup can be seen in Figure 27.

Figure 27: Construction of the autoclave used in the experiments

After 90 min, the autoclave was cooled down to 60 °C and afterwards depressurized and opened. Subsequently, the suspension was filtered. The filtration cake was first rinsed and afterwards washed in water for 45 min to remove any adhering solution that could contain chlorine or sodium. The resulting suspension was filtrated again and finally put to dry at 110 °C.

- Results

The results of the hydrometallurgical treatment of the TBZC intermediate product in the autoclave can be seen in Table 15. It was possible to reduce the content of chlorine to under 0,1 %. However, as a result of the treatment, some of the sodium remained in the product bringing the overall Na-content to 0,21 %. This contamination with Na can likely be significantly reduced by a more sophisticated method of washing or a more accurate dosage of Na_2CO_3. When weighing on the day after the experiment the filtration cake apparently was not yet completely dried, which resulted in an implausible mass of the product. Therefore, the creation of a mass balance for the experiment was not possible. In the elemental analysis, however, it can be seen that it was possible to reduce the chlorine content of the former TBZC under 0.1 %.

Table 15: Analysis results of the input and output for the soda leaching in the autoclave (AMCO)

Detail	Input	After leaching at 125 °C
Zn [%]	46.5	56.0
Cl [%]	10.0	<0.1
Na [%]	0.0	0.2
Mass [%]	100.0	101.7

Due to the missing mass balance for this experiment, it will also not be possible to calculate the yield of zinc the chlorine extraction as well as the separation factor.

3.3.5 Interpretation of results of hydrometallurgical treatment

As a result of the higher input of soda at higher temperatures, the sodium content in the solid product after filtration and washing was also higher. This can likely be avoided in the future by using a more thorough washing process. While it can be seen that there was almost no extraction of chlorine at the lower temperature of around 30 °C, it is shown that with increasing temperature, the efficiency of the dechlorination is also increasing. The experiment conducted at 80 °C showed a great outcome regarding the final level of chlorine of only 0.2 %.

In order to make the comparison to the pyrometallurgical route easier, the separation factor according to equation (13) as well as the zinc yield and the chlorine extraction have been calculated and can be seen in Table 16.

Table 16: Chlorine extraction, zinc yield and separation factor for the three experiments

	30 °C	**60 °C**	**80 °C**
Chlorine extraction [%]	4.4	35.6	97.5
Zinc yield [%]	97.5	101.6	100.6
Separation factor [-]	0.02	0.37	0.98

Differently to what was suggested by the thermodynamic calculations, dechlorination did not work at lower temperatures with a removal of only 4 %. The cause of this has not yet been fully determined, but is likely a kinetic aspect. For the experiment at 60 °C, it can be seen that 35.6 % of chlorine was extracted. This means that some dechlorination took place, but was either too slow or equilibrium was reached too early. Here, further experiments would be needed for example using a longer reaction time. Another possibility for improvement is conducting the leaching treatment in two steps, as it is industrially done. [31] This means that after the initial soda leaching, the solid fraction is leached again. Therefore, it is possible to reach further dechlorination, after the equilibrium in the first leaching step was reached.
When looking at the hydrometallurgical experiments it becomes clear that the higher temperature was advantageous for chlorine extraction. The best results were achieved at 80 °C, with a separation factor of 0.98. While there were problems with calculating the mass balance in the last experiment in the autoclave, the results during the last soda leaching experiment were already satisfactory. The marginal improvement of lowering the chlorine content another 0.1 % does not make up for the more complicated process when using an autoclave.

4 Color change of zinc oxide due to thermal treatment

As already mentioned in chapter 2, the appearance of the ZnO as a white powder is an important sign of quality. While the initial precipitate had a bright white color, the color shifted toward a light yellow color after the thermal treatment. Although, it was first believed that this shift was due to impurities in the precipitation product, the shift to green yellow has also been described by Moezzi, Cortie et al. who have used pure chemicals in their experiments. [33]

The color change of zinc oxide is based on different mechanisms that change the optical energy of the oxide and result in absorption of blue and UV light. This can, among other things, be a consequence of changes in the crystal size or crystal defects [57, 58]. Based on the temperature and the atmosphere during the thermal treatment, this change in energy can have different causes, which can either be reversible or irreversible. For the quality of the ZnO powder only the irreversible change of the optical energy is relevant. The first possible cause for change of the absorption energy is the decomposition of zinc oxide leading to the formation of an under-stoichiometric compound with an excess of zinc. While this change can be reversible for lower temperatures, it stays permanent when heating ZnO up over 0.25 T_m. [59–61] Based on the maximum temperature as well as the cooling rate, different types of under-stochiometric ZnO can be formed in small quantities, which as a result have an impact of the luminescence and the absorption peak of the material. [61]

Another cause for the change in its optical properties is the size increase of particles during heating. It has been found that the optical properties barely changed for temperatures under 600 °C. However, upon heating above 600 °C, the optical energy of the ZnO powder irreversibly changed, which has been linked to an increase in crystal size, verified by XRD measurements. This increase in crystal size in consequence altered the optical energy gap of the material. [57]

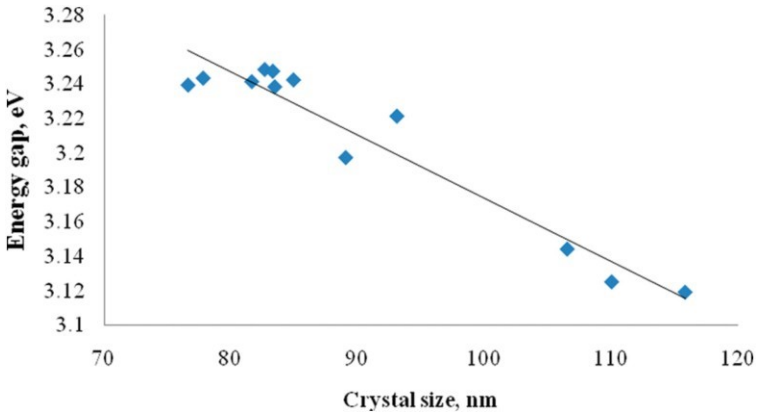

Figure 28: Influence of the crystal size on the band energy gap in zinc oxide [57]

The particle growth of zinc oxide upon thermal treatment has also been investigated and even for short periods of annealing at 500 °C the effect was visible on the SEM. [29]
It is also important to note that zinc oxide changes its color upon mechanical treatment such as grinding, due to defects in the crystal lattice. Therefore, it is not possible to reverse the crystal growth by crushing. [62]
When looking at
Figure 20, it can be noticed that the color change is different based on the atmosphere during the thermal treatment. In the two experiments conducted under synthetic air the color turned to a grey/green tone, however, when using an atmosphere without oxygen it could be noticed that it turned yellow. This is in line with the previously presented findings. The greyish discoloration shown by the samples treated in synthetic air seems to be linked to crystal growth. Additionally, it appears that when using a nitrogen atmosphere, an under-stochiometric zinc oxide is formed, causing a yellow discoloration similar to what has been determined by Van Craeynest. In Figure 29, the SEM pictures of two samples after thermal treatment in different atmospheres are compared.

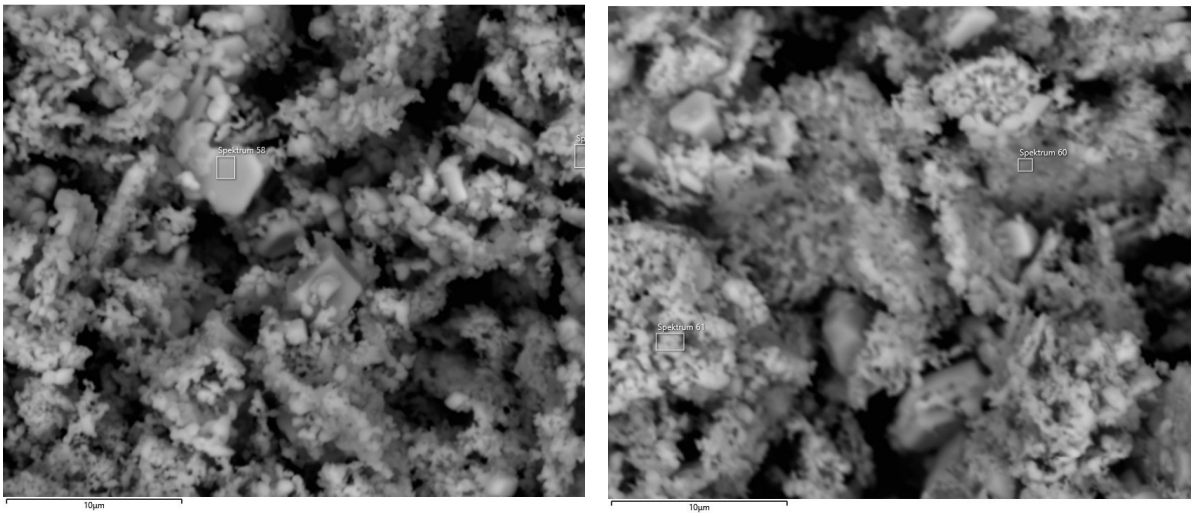

Figure 29: Comparison of the SEM pictures of the thermally treated samples, (left Nitrogen H_2O, right syn air H_2O)

It can be seen that the previously layered structure as seen in Figure 8 has been destroyed and replaced by a porous structure, similar to what has been reported in a paper of Chinese researchers. [6] Furthermore, it is visible that the atmosphere during thermal treatment has little to no influence on the structure after heating.

5 Alternative precipitation route

In the following, an alternative route for the extraction of zinc oxide from zinc and iron bearing residues is assessed by conducting a tentative experiment. In contrast to the original process route $Mg(OH)_2$ is not being used in the several precipitation steps in order to raise the pH level. This has the advantage that the precipitate cannot be contaminated by magnesium. Furthermore, next to the precipitation of iron, further steps to purify the solution are added. These are the cementation of lead as the second purification step as well as the precipitation of calcium as gypsum in the third purification step. The flow chart for this possible alternative route can be seen in Figure 30.

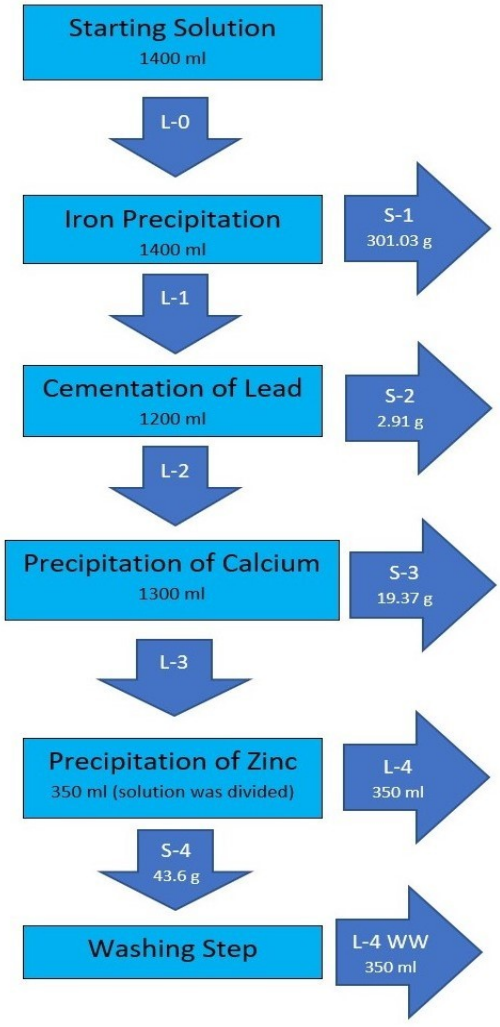

Figure 30: Flow sheet for the alternative precipitation route

Differently to the original process, the zinc will be precipitated by first raising the pH level with NH_4OH and subsequently injecting CO_2 into the solution. As a result, the zinc is supposed to be precipitated as zinc carbonate in contrast to $Zn(OH)_2$, which turned out to be $Zn_5(OH)_8Cl_2$

in the original process. As zinc is precipitated as carbonate, no zinc losses are to be expected upon calcination, contrary to the original route where TBZC is produced.

5.1 Preparation of the starting solution

Prior to the alternative precipitation experiment the starting solution was generated. The goal was to produce about 2.5 l of the solution that is present right after hydrolysis of the leachate. For this, 968 g of H_2O and 1 536 g of HCl were mixed in a 5 l beaker and heated to 60 °C. Afterwards, different metal oxides were dissolved in the solution in order to create a synthetic leaching solution. In Table 17, the added masses of the different metal oxides are summarized. The preparation of this solution was analogous to the preparation of the solution for the original route, as reported in chapter 3.1.2.

Table 17: Utilized metal oxides for the preparation of the solution for the alternative precipitation route

MeO	Calculated weight [g]	Real weight [g]
MnO	11.72	11.96
PbO	1.60	1.65
Fe_2O_3	3.30	3.66
CaO	20.72	21.49
ZnO	622.08	623.61

Afterwards, the solution was split into two parts, with one part going into the conventional $Mg(OH)_2$ precipitation route, while the other part is further processed via the alternative precipitation route. The starting volume for the alternative route was 1 400 ml out of the total 2 500 ml solution which have been prepared. The starting solution had a pH of 3.64.

5.2 Iron precipitation

The first step in the cleaning of the leachate was the precipitation of iron. In order to make a full precipitation possible, a small quantity of H_2O_2 was added oxidizing any present Fe^{2+} ions. As a precipitation chemical 25 % $NH_4(OH)$ is used. By adding $NH_4(OH)$ the pH level of the solution was raised to 5.0 to make the formation of the iron precipitate possible. $NH_4(OH)$ was slowly added to the solution with a total mass of 275.94 g over the time of one hour. During the addition of $NH_4(OH)$, the brown color of the solution turned to a lighter brown as can be seen in Figure 31.


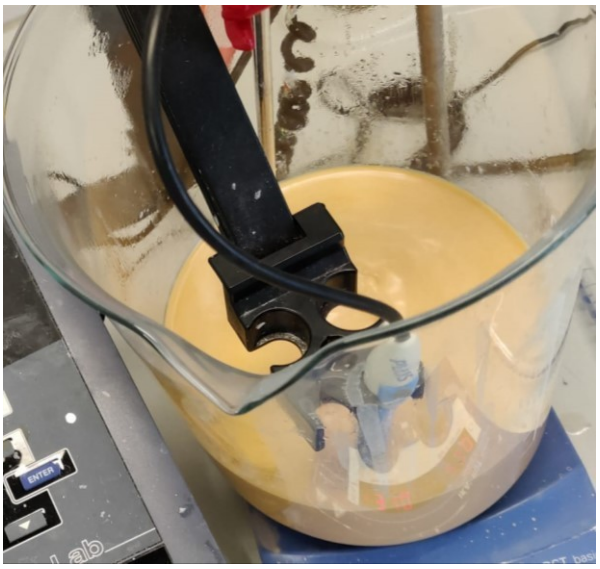

Figure 31: Color of the solution after the addition of H_2O_2 at a pH of 3.6 (left) and 4.7 (right)

After reaching the targeted pH level, the solution is left to stand for 15 min allowing for a full completion of the reaction. Before starting the precipitation, a sample L0 is taken with a volume of about 20 ml. During filtration and when rinsing the empty beaker, it was noticeable that compared to the sandy texture of the precipitate in the normal process, the precipitate from the alternative route had more of a muddy texture. As a result, even after the filtration was completed the cake seemed to have a higher water content compared to the normal route, resulting in losses by adherent solution. Because of the muddier texture, the filtration took longer with a total time of 22 min. After the filtration, a sample of the filtrate (L1 – 20 ml) and the cake (S1) were taken. Due to the longer filtration time, the solution has cooled down to about 25 °C, which caused a white precipitate, possibly zinc hydroxide, to form inside the solution. This can be seen in Figure 32 on the left side.

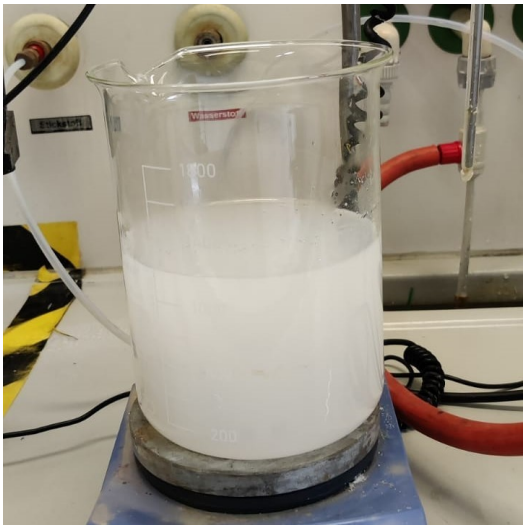
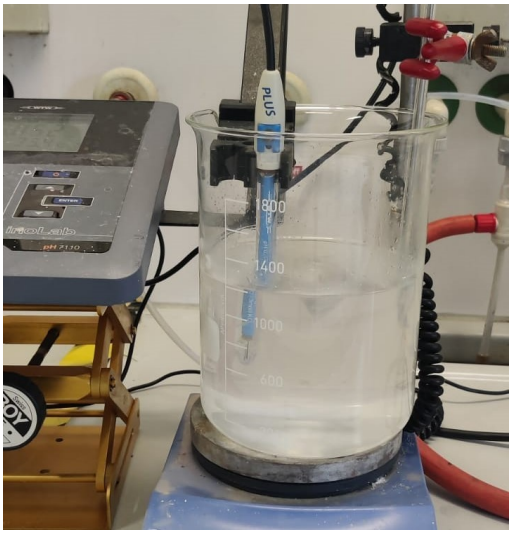

Figure 32: The solution before (left) and after (right) redissolving the zinc precipitate

The zinc precipitate was dissolved again after adding 22 ml of HCl and reheating the solution to 60 °C. It was also observed that the pH level of the filtrate was higher (5.2) than the pH level of the solution before the filtration. Subsequently to the filtration, the filtration cake was put into a drying cabinet at 110 °C. After 40 min the solid particles in the mud started to sediment. In Figure 33 it can be seen how much liquid was carried over into the filtrate as a consequence.

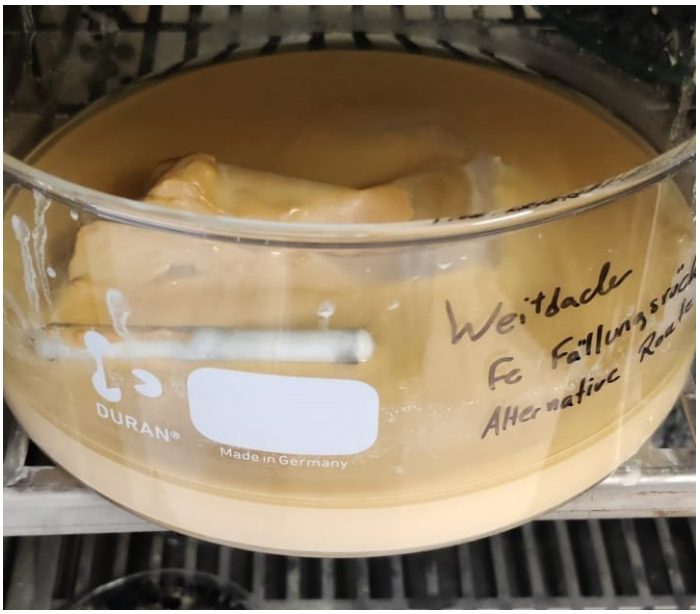

Figure 33: Filtration cake after the being left to rest for 40 min

5.3 Cementation

The goal of the cementation step is the removal of noble impurities such as lead or cadmium. The cementation was conducted at a temperature of 35 °C after the zinc precipitate in the filtrate was redissolved. Upon the addition of 2.5 g of zinc powder, the pH level directly declined to 4.27 and afterwards slowly raised to 4.5 over the course of 10 min. After being added to the solution, the zinc powder almost immediately turned black and accumulated into lumps. In order to make a complete reaction possible, these lumps were then continuously crushed with a stirring rod. About 20 min after the addition of the zinc powder, the filtration was started. Again, two samples were taken. The first one of the filtrate (L2) and the other one of the solid filtration residue (S2). The solid fraction, the so called cementate, is depicted in Figure 34.

Figure 34: Solid residue of the filtration step after the cementation of lead

After the filtration, the volume of the remaining solution was 1.3 l at a pH level of 4.4. The solution directly was processed further in the precipitation of calcium.

5.4 Precipitation of calcium

In this step, calcium is precipitated as gypsum by the addition of $(NH_4)_2SO_4$. Firstly, 25.44 g of $(NH_4)_2SO_4$ were dissolved in water and then added to the solution. In the beginning, the solution showed no reaction upon the addition of $(NH_4)_2SO_4$, although it was assumed that the precipitation would take place in a fast reaction. Therefore, it was believed that there was no calcium left in the solution to be precipitated. As a result, a liquid sample (L3-b) was taken and the solution was prepared for storage. However, it was noticed that small white flakes started to form in the solution after about 10 min. While this could have been attributed to the precipitation of zinc due to the sinking temperatures, it is more likely that it was simply a delayed precipitation of the gypsum. The flaky appearance seen in Figure 35 typically is a sign of gypsum.

Figure 35: Appearance of the precipitate after addition of $(NH_4)_2SO_4$

Upon the identification of the white precipitate flakes, the solution was filtered again. A sample of the solid cake (S3) and of the filtrate (L3) was taken. After this step, the filtrate was filled in a volumetric flask and stored until the next step for about one week.

5.5 Alternative precipitation of zinc compound

In the final step of the alternate process the zinc intermediate product is precipitated. The solution was split again, to have a backup in case something unforeseen happens. The starting volume for the experiment was 300 ml. The solution was put into a beaker of 1 l volume, which was placed on a stirring plate. It is important to use a high beaker, in order to prevent spilling due to the agitation from the gas flushing. The experimental setup can be seen in Figure 36. A glass frit was used for the injection of the CO_2. During the whole process, the pH level and the temperature were measured via a pH-meter with an integrated thermometer. No heating was done, therefore any raises in temperature documented are due to reaction heat. At t=0 min the first drops of 25 % NH_4OH were added. Subsequently, the pH level of the solution was lifted to at least 7 under continuous stirring. After reaching the target pH level, CO_2 was injected into the solution using a gas frit.

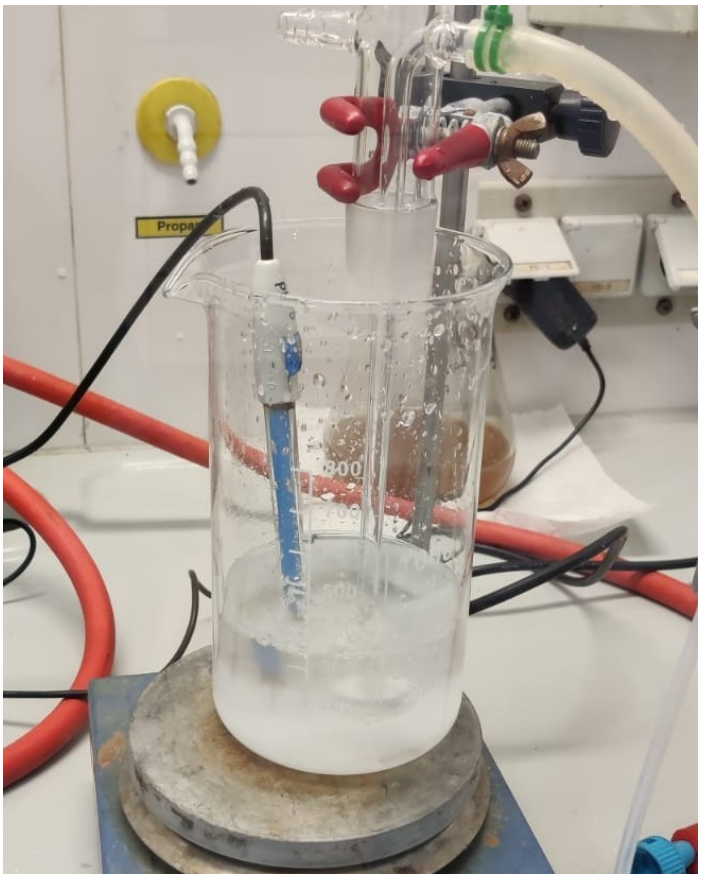

Figure 36: Experimental setup during the precipitation of zinc compound

The addition of NH_4OH over time, the development of pH and temperature are summarized in Table 18.

Table 18: Documentation of the change in temperature and pH upon the addition of NH_4OH

Time [min]	Temperature [°C]	pH	NH_4OH added [g]
0	24.4	5.2	0
10	24.7	5.5	6.5
20	28.6	6.2	41.5
30	33.7	6.4	54.5
40	36.5	7.1	94.5

The first formation of white precipitate was observed at around 30 min and a pH level of 6.4, as it is shown in Figure 37. In order to allow for a complete precipitation of zinc from the solution after reaching the pH of 7, the solution was left for reaction for another hour, while prolonged flushing with CO_2.

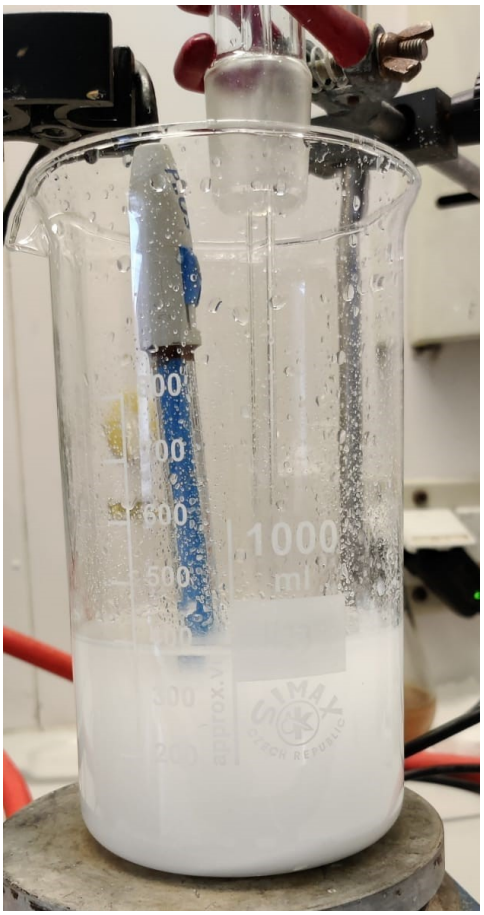

Figure 37: First formation of white precipitate after approximately 30 min of treatment time

After about 40 min, a reduction in gas flow through the solution was observed. In order to offset this and establish the normal gas flow, the pressure was increased. However, this caused one of the tubes to expand slowly, which is why the pressure was reduced again. When investigating the cause of this pressure buildup, it became noticeable that the porous ceramic of the glass frit was clogged by white precipitate, which can be seen in Figure 38 on the left.

Figure 38: Clogged gas frit due to the precipitation of zinc on the porous ceramic (left) precipitate sticking to the bottom of the beaker (right)

Due to this, the glass frit was changed to a simple glass tube, which resulted in bigger as well as fewer bubbles being produced. After additional 20 min, the suspension was filtrated. One sample of the zinc precipitate (S-4) and of the filtrate (L-4) were taken. Some white precipitate has been found to stick to the bottom of the beaker and could not be removed by simply scratching it off with a spatula. The remaining adhering precipitate at the bottom can be seen in Figure 38 on the right side.

After the filtration, the cake was rinsed and finally suspended in purified water. Subsequently, the suspension was heated to 60 °C while stirring. After reaching the target temperature, it was held for 10 min upon one final filtration step. This step was used to remove adhering solution from the solid fraction. One final sample (L-4WW) was taken of the washing water.

5.6 Analysis and results of the individual process steps

The composition of the starting solution after dissolving the oxides can be seen in Table 19. The volume in the beginning was 1.4 l. It is noticeable that a small part of the iron in the solution is present as divalent iron. This makes the addition of hydrogen peroxide necessary in order to oxidize it to trivalent iron before its precipitation. Overall, 376.8 g of zinc were present in the solution at the start of the experiment.

Table 19: Chemical Analysis of the starting solution (sample L-0)

Element	Concentration [mg/l]
Ca	7 200
Mn	4 800
Pb	800
Zn	269 000
Fe^{2+}	6
Fe^{3+}	1 137

5.6.1 Precipitation of iron

The volume of filtrate after the precipitation of iron was about 1 200 ml. It can be seen that the removal of iron was successful with both the concentrations of divalent as well as trivalent iron in the filtrate below 2 mg/l. The total weight of the dried filtration cake was 301.39 g and its composition is listed in Table 20. It can be seen that the main fraction of the filtration cake consisted of zinc, resulting in zinc losses of 164.9 g in this step. For industrial scale this makes a further processing of this mass stream mandatory. After drying, the consistency of the filtration cake changed from muddy into a hard solid. This stands in contrast to the sandy consistency of the filtration cake from the original route. After drying, it turned hard which made it impossible to grind by hand.

Table 20: Chemical Analysis of precipitate and filtrate after the precipitation of iron (sample L-1 & S-1)

Element	Filtrate [mg/l]	Precipitate [%]
Ca	6 100	0.7
Mn	3 900	0.5
Pb	600	0.1
Zn	129 000	54.7
Fe^{2+}	<2	<0.5
Fe^{3+}	<2	<0.5

5.6.2 Cementation of lead

The volume of the filtrate after the cementation and subsequent filtration was 1.3 l. While the concentration of lead in the solution was significantly reduced, a complete removal was not possible and 0.33 g/l of lead remained in the solution. In Table 21, the chemical analysis of the cementate is shown.

Table 21: Chemical analysis of the filtrate and cementate after the removal of lead (sample L-2 & S-2)

Element	Filtrate [mg/l]	Cementate [%]
Ca	5 800	-
Mn	3 700	-
Pb	300	7.5
Zn	124 000	86.8

The total weight of the dried cementate was 2.91 g. While some lead was removed, with a zinc content of 86.8 % the cementate still mainly consists of zinc due to required excess amount of metallic zinc dust for this process step.

5.6.3 Precipitation of calcium as gypsum

The total volume of filtrate after the removal of calcium was 1.25 l. As mentioned in the experimental description, there were some irregularities during this step. While first it seemed as if the reaction had not taken place, it simply had happened a lot slower than expected. Still, the remaining concentration of calcium after the reaction was relatively high, as shown in Table 22.

Table 22: Chemical analysis of the filtrate and precipitate after the removal of calcium as gypsum (sample L-3 & S-3)

Element	Filtrate [mg/l]	Precipitate [%]
Ca	4 800	2.6
Mn	3 300	-
Zn	97 000	43.6
Cl	-	29.5

The total weight of the calcium filtration cake was 19.37 g. It again can be seen that while some calcium is present in the solid, it mainly consists of zinc with a zinc content of 43.6 %.

5.6.4 Precipitation of zinc compound

The weight of the dried zinc precipitation product was 43.6 g. This equates to 155.71 g projected for the whole solution if the previous filtrate had not been split. The chemical composition of the zinc precipitate can be seen in Table 22.

Table 23: Chemical analysis of the zinc precipitate (sample S-4)

Element	Concentration [%]
Ca	3.3
Fe	<0.01
Mn	2.8
Pb	0.2
Zn	61.3
Cl	4.3

If the numbers of the fraction of the solution are projected for the full volume of filtrate in the previous step, the zinc yield over the entire alternative precipitation route can be calculated. Overall, big losses of zinc occurred in almost every step, bringing the overall zinc yield to 25.3 %. As this was only a tentative trial to verify the concept in general, the overall yield can still be improved in future experiments.

5.7 Characterization of the zinc precipitate from the alternative route

A SEM picture of the zinc precipitate from the alternative route can been seen in Figure 39. As expected, the structure does not resemble the typical TBZC structure anymore.

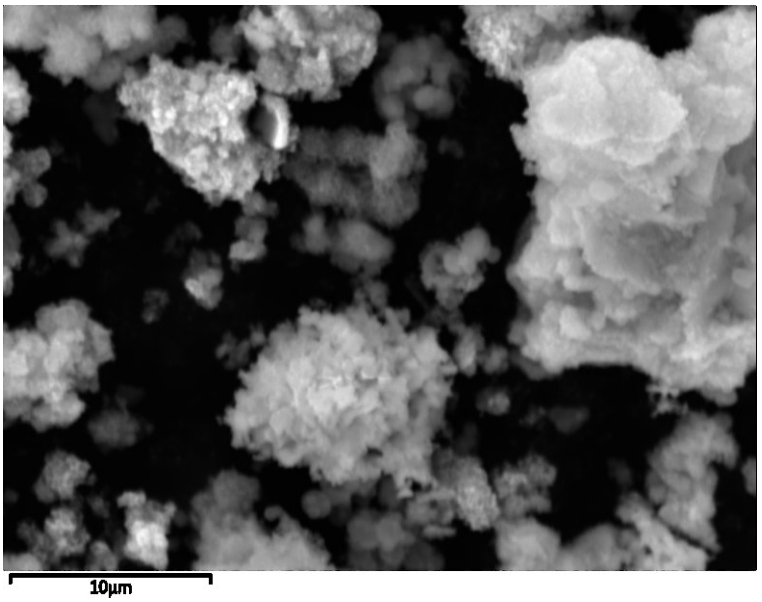

Figure 39: SEM picture of the zinc precipitate from the alternative route

In Table 24, the chemical compositions of the filtrate after the zinc precipitation step as well as the washing water is shown. The final volume of filtrate was 350 ml.

Table 24: Chemical analysis of the filtrate after the extraction of zinc (sample L-4) and the washing water (sample L-4 WW)

Element	Filtrate [mg/l]	Washing water [g/l]
Ca	570	-
Mn	5	-
Pb	3	-
Zn	20 800	2.1
Fe^{2+}	<2	-
Fe^{3+}	<2	-
Cl	-	20.6

The volume of the washing water was 650ml. With the washing, it was possible to remove some of the adhering hydrochloric acid from the solid fraction, and consequently reducing the chlorine content.

Afterwards, a thermal analysis was conducted for the product of the alternative precipitation route. The resulting TG/DTA curve gained in the thermal analysis is given in Figure 40.

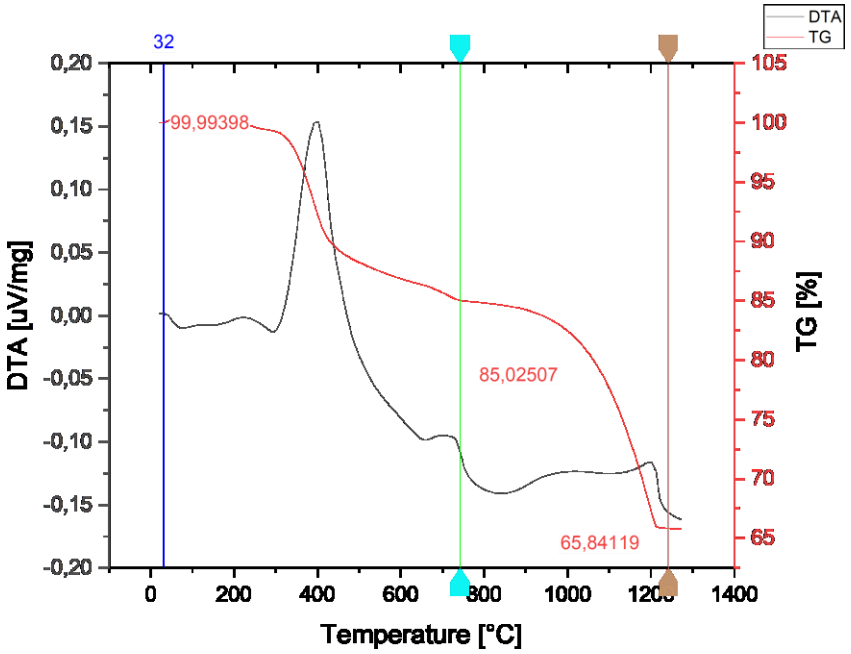

Figure 40: TG/DTA curve of the alternative precipitate

It is visible that the majority of the mass loss occurred in two steps, with the first one starting at around 300 °C. The mass loss in the first phase is equal to about 12.5 % of the total mass. The initiation of the second mass loss (22 %) is detected at 700 °C. The total mass loss is equal to 34.87 %.

6 Discussion

In the following subchapters, the different investigated options for dechlorination are compared and advantages as well as disadvantages are pointed out. Furthermore, the results of the alternative precipitation route are investigated and potential room for improvement is discussed.

6.1 Dechlorination

Both the thermal and the hydrometallurgical treatment options were successful in removing chlorine from the precipitation intermediate product. The separation factors are used for the comparison of the different paths, also taking the zinc losses during the process into account. Additionally, economic as well as ecological factors are considered.

As can be seen in Table 25, the highest separation factor was achieved in the third soda leaching experiment at 80 °C. The main advantage of the hydrometallurgical route were the low zinc losses compared to the thermal treatment. However, it can be said that due to its high volatility during thermal treatment, the extraction of chlorine was more consistent. Nevertheless, both of these treatment methods for dechlorination still show potential for optimization by changing the various input parameters.

Table 25: Comparison of the different separation factors for dechlorination experiments

Experiment	Zinc yield	Separation factor
Thermal treatment syn. air	86.1	0.85
Thermal treatment steam/N_2	104.4	0.99
Thermal treatment steam/syn. air	102.9	0.99
Soda leaching 30 °C	97.5	0.02
Soda leaching 60 °C	101.6	0.37
Soda leaching 80 °C	100.6	0.98
Soda leaching autoclave	-	-

When solely looking at the process side, the simple clinkering of the TBZC seems to be the better option. The thermal treatment of the precipitation product can possibly be included in the calcination step which is already part of the process.

During the thermal treatment of the precipitate, one step is sufficient compared to the hydrometallurgical process where subsequently to the soda leaching a washing step as well as a calcination needs to take place. Another positive aspect of the thermal treatment of TBZC is that no further chemicals are required, while for the hydrometallurgical process at least sodium carbonate and possibly NaOH are needed.

Another important aspect to consider are possible residues which are produced in the process. In the thermal treatment, filter dust is produced as a byproduct. This filter dust mainly consists of zinc, chlorine as well as other volatile impurities and can likely be recycled into the process by soda leaching. For the hydrometallurgical removal of chlorine, waste water treatment is required following the leaching and washing of the product. Additionally, CO_2 is emitted during calcination of the soda leaching product. When using thermal treatment, a completely carbon neutral process is possible if electrothermal heating is used.
Furthermore, other impurity elements such as lead or cadmium, which are very big problems for product quality, can be removed by volatilization through thermal treatment. [10, 11, 17, 31]

6.2 Color change

According to what has been found about the irreversible change in color for zinc oxide upon thermal treatment, it is important to limit the maximum temperature to under 600 °C to avoid crystal growth. [57] While the maximum temperature to avoid the formation of an under-stochiometric zinc oxide is around 500 °C, this color change can also reversed by an oxygen rich atmosphere and slow cooling. [59] Based on the work of Garcia-Martinez, the thermal decomposition of TBZC at a heating rate of 1 °C/min is completed around 447 °C. This means that there theoretically a way of thermally removing the chlorine from the material, while keeping a satisfactory zinc yield as well as avoiding color change in the product, exists.

6.3 Alternative precipitation route

While the precipitation of iron with NH_4OH was successful in the alternative route, there were some issues with the cementation of lead as well as the removal of calcium. A comparison between the zinc precipitate obtained from the original route and the precipitate from the alternative precipitate is shown in Table 26.

Table 26: Comparison between the products of the alternative and the original processing route

Element	Zinc product [alternative]	Zinc product (TBZC) [original]
Ca [%]	3.3	<0.02
Fe [%]	<0.01	<0.02
Mn [%]	2.8	0.3
Pb [%]	0.2	<0.02
Zn [%]	61.3	56.9
Cl [%]	4.3	12.3
Mg [%]	-	2.7

When using the alternative route, the concentration of chlorine in the zinc precipitate was significantly lower compared to the original route. With a chlorine content of 4.3 % and a zinc content of 61.3 %, a maximum of 32 % of all zinc can stoichiometrically be contained as part of TBZC. In contrast to that, in the product of the original precipitation route 100 % of the Zinc in the solid existed as part of TBZC, as was previously shown.

During the cementation of lead, it has been observed that a lot of zinc remained in the cementate despite lead still being partly in the solution. Normally, zinc would only be in the cementate if all the more noble metals were reduced. Therefore, it seems that some of the zinc was prevented from reaction due to a layer of product over it. Overall, this step had the advantage that some of the lead was removed without adding another impurity. Considering that lead is one of the most critical elements concerning the quality of zinc oxide, this is a crucial achievement. For the removal of calcium further investigation is necessary. The filtration cake, which normally should have been gypsum, mainly consisted of zinc compound while the majority of calcium stayed in the solution.

Furthermore, it can be seen that the content of manganese is 10-times higher when using the alternative route. The removal of manganese was planned as part of the iron precipitation step, however, little to no removal of manganese occurred in this step. The cause of this still has to be determined.

Based on the thermal analysis and the results of the chemical analysis, it is now possible to identify the different zinc containing compounds in the precipitate. A rough calculation of the different compounds in the precipitate of the alternative route is summarized in Table 27.

Table 27: Fractions of the different zinc compounds based on thermal as well as chemical analysis

Compound	Fraction of total zinc in compound [%]
$ZnCl_2$	6.5
$ZnCO_3$	75.0
$Zn(OH)_2$	18.5

It can be assumed that the chlorine found in chemical analysis is part of $ZnCl_2$ and will be evaporated as such at around 730 °C. The form of the TG curve for the second mass loss is characteristic of the evaporation of chlorides. A complete evaporation of chlorine as $ZnCl_2$ would result in a mass loss of 16.5 %.

The remaining mass loss is 18.3 % and is assigned to the evaporation of water and CO_2 from either $Zn(OH)_2$ or $ZnCO_3$. According to calculations, the share of CO_2 liberation of the second mass loss is 80 % while the evaporation of water is 20 %. Based on this, the mass fraction of $ZnCO_3$ and $Zn(OH)_2$ can be approximated under the assumption that no other reactions

caused the mass loss. A more accurate identification of compounds in the precipitate might be possible through XRD.
Overall, with 6.5 % of the total zinc bound as zinc chloride, the possible loss during calcination is significantly smaller compared to a maximum mass loss of 20 % when TBZC is formed.

7 Summary and future outlook

To conclude, it can be said that both the hydrometallurgical and the thermal path for dechlorination look promising. It was possible to realize separation factors of over 0.9 for both routes, removing chlorine while still keeping a satisfactory zinc yield. For the thermal treatment, pyrohydrolysis of TBZC in both synthetic air as well as nitrogen atmosphere were successful. Meanwhile, in the hydrometallurgical route it was possible to achieve a separation factor over 0.9 for both the soda leaching at 80 °C and the soda leaching in the autoclave at 120 °C. However, not successful was the soda leaching at 60 °C, the soda leaching experiment at 30 °C as well as the thermal treatment without water vapor. For these parameters, further investigation is advisable as both of them offer benefits compared to the processes which already achieved better results. On the one hand, a potential for improvement certainly are low heating rate experiments for the thermal treatment. On the other hand, for the soda leaching at 60 °C better separation could be achieved by a longer reaction time or a two-step leaching process.

The discovery of the color change in the product upon heating is another problem that was discovered and still needs to be resolved. This causes an issue as the pure white color is an important quality aspect for zinc oxide, especially in the ceramics industry. The causes for the change in color have already been discussed and both of the known causes are linked to overstepping a certain temperature in order for the change in color to take place. Therefore, in further experiments it could be determined whether dechlorination can be completed without overstepping that critical temperature of 600 °C. Furthermore, the content of manganese of the TBZC that was synthetically produced in the laboratory exceeded the required specifications for most of the applications. This, however, cannot be solved by thermal treatment or soda leaching, but has to be addressed in an additional cleaning step prior to the precipitation.

The production of a precipitation product with a lower chlorine content over the alternative precipitation route was also successful. While the overall yield of zinc was still pretty low, it was possible to decrease the content of lead by cementation. Additionally, a way of iron precipitation without using $Mg(OH)_2$ and therefore adding magnesium as an impurity has been discovered. While the selective removal of calcium did not show the expected results, further optimization is possible with the knowledge from the tentative trial. Even if the alternative precipitation route is not pursued further, the integration of additional cleaning steps into the original route looks like a promising way to optimize product quality. Overall, lead and manganese seem to be the biggest problems concerning product quality, when looking at the specifications for the use in different markets. For the removal of lead, cementation also proved to be an effective measure which could be implemented into the original route.

8 References

[1] EverZinc: Overview Applications. Internet: https://www.everzinc.com/en/ (Zugriff: 03.02.2022).

[2] Stefan Steinlechner J. A.: Hydro- and Pyrometallurgical Options for the Upgrading of Low Grade Secondary Zinc Oxides. European Metallurgical Conference EMC-2011 (2011) online proceedings.

[3] Timothy van Audenaerde: Steel Demand Beyond 2030, Paris (28.09.2017).

[4] Liebman M.: The Current Status of Electric Arc Furnace Dust Recycling in North America. In: Stewart, D. L., Daley, J. C., Stephens, R. L. (Hg.): Recycling of Metals and Engineercd Materials. Hoboken, NJ, USA: John Wiley & Sons, Inc, 237–250.

[5] International Zinc Association: ZnO and Zinc Chemicals Market Update. 2016 International Zinc Oxide Industry Conference.

[6] Zhang Y. et al.: Large scale synthesis of hexagonal simonkolleit nanosheets for ZnO gas sensors with enhanced performances. Materials Letters, 186 (2017), 7–11.

[7] Khan S. B. et al.: An assessment of zinc oxide nanosheets as a selective adsorbent for cadmium. Nanoscale research letters, 8 (2013), 377.

[8] ASTM International. ASTM D4315 - 94 Standard Test Methods for Rubber Compounding Material-Zinc Oxide.

[9] ISO. ISO 9298 - Rubber compounding ingredients - Zinc Oxide - Test methods.

[10] Dr. Stefan Steinlechner: Amelioration and market strategies for zinc oxide with focus on secondary sources.

[11] EverZinc: Tyres & Rubbers. Internet: https://www.everzinc.com/en/tyres-rubbers (Zugriff: 11.09.2021).

[12] EverZinc: Zinc Oxide Red Seal - Technical Data Sheet.

[13] Numinor: Zinc Oxide White Seal - Technical Data Sheet.

[14] EverZinc: GMP Zinc Oxide - Technical Data Sheet.

[15] Caterina Benigni: Zinc oxide from steel mill dust - A wide range of opportunities. European Steel Technology and Application Days (2017) online proceedings.

[16] ROSENTHAL A. B. und S. H. GAROFALINI: Structural Role of Zinc Oxide in Silica and Soda-Silica Glasses. Journal of the American Ceramic Society, 70 (1987), 821–826.

[17] EverZinc: Glass & Ceramics. Internet: https://www.everzinc.com/en/glass-ceramics (Zugriff: 11.09.2021).

[18] ZoChem: Recommended Products by Application. Internet: https://www.zochem.com/products/recommended-products-by-application/ (Zugriff: 11.09.2021).

[19] Bellit: Zinc Oxide Green Seal - Technical Data Sheet.

[20] ZoChem: Zinc Oxide Grade 500 - Technical Data Sheet.

[21] ZoChem: Zinc Oxide Grade 124G - Technical Data Sheet.

[22] ZoChem: Application: Micronutrients / Animal Nutrition.

[23] European Food Safety Authority: Scientific Opinion on the safety and efficacy of tetra-basic zinc chloride for all animal species. EFSA Journal, 10 (2012), 2672.

[24] THE EUROPEAN PARLIAMENT AND THE COUNCIL OF THE EUROPEAN UNION – EN Official Journal of the European Communities 30.5.2002L 140/10 DIRECTIVE 2002/32/EC OF THE EUROPEAN PARLIAMENT AND OF THE COUNCIL of 7 May 2002 on undesirable substances in animal feed (2002).

[25] ZoChem: Zinc Oxide Grade 500WSA - Technical Datasheet.

[26] Bryn Harris C. W.: WO 2020/107122 A1 – PROCESS FOR THE RECOVERY OF VALUE METALS FROM ZINC-BEARING ORES, CONCENTRATES, INTER¬ MEDIATES AND WASTES.

[27] Zhang und K. Yanagisawa: Hydrothermal Synthesis of Zinc Hydroxide Chloride Sheets and Their Conversion to ZnO. Chemistry of Materials, 19 (2007), 2329–2334.

[28] Tanaka H. et al.: Synthesis and characterization of layered zinc hydroxychlorides. Journal of Solid State Chemistry, 180 (2007), 2061–2066.

[29] Rostas A. M. et al.: Electron paramagnetic resonance and microstructural insights into the thermal behavior of simonkolleite nanoplatelets. Physical chemistry chemical physics : PCCP, 22 (2020), 9503–9512.

[30] 3rd Seminar on Networking between Zinc and Steel: Options for Halogen Removal from Secondary Zinc Oxides (2011) online proceedings.

[31] Antrekowitsch J. und D. Offenthaler: Die Halogenproblematik in der Aufarbeitung zinkhältiger Reststoffe. BHM Berg- und Hüttenmännische Monatshefte, 155 (2010), 31–39.

[32] Sinclair R. J.: The extractive metallurgy of zinc. In: Spectrum series / Australasian Institute of Mining and Metallurgy, Band: 13. AusIMM, Carlton, Vic. (2005).

[33] Moezzi A., M. Cortie und A. McDonagh: Transformation of zinc hydroxide chloride monohydrate to crystalline zinc oxide. Dalton transactions (Cambridge, England : 2003), 45 (2016), 7385–7390.

[34] Li Z. et al.: Dechlorination of Zinc Oxide Dust from Waelz Kiln by Microwave Roasting. High Temperature Materials and Processes, 34 (2015) online proceedings.

[35] Wei Y. et al.: Dechlorination of zinc dross by microwave roasting. Journal of Central South University, 21 (2014), 2627–2632.

[36] Kozawa T. et al.: Effect of water vapor on the thermal decomposition process of zinc hydroxide chloride and crystal growth of zinc oxide. Journal of Solid State Chemistry, 184 (2011), 589–596.

[37] Gorodylova N. et al.: Thermal transformation of layered zinc hydroxide chloride. Journal of Thermal Analysis and Calorimetry, 127 (2017), 675–683.

[38] Srivastava O. K. und E. A. Secco: Studies on metal hydroxy compounds. I. Thermal analyses of zinc derivatives ϵ-Zn(OH) 2 , Zn 5 (OH) 8 Cl 2 .H 2 O, β-ZnOHCl, and ZnOHF. Canadian Journal of Chemistry, 45 (1967), 579–583.

[39] Rasines I. und J. I. Morales de Setién: Thermal analysis of β-Co2(OH)3Cl and Zn5(OH)5Cl2 · H2O. Thermochimica Acta, 37 (1980), 239–246.

[40] Hoffman J. W. und I. Lauder: Basic Zinc Chlorides. Australian Journal of Chemistry, 21 (1968), 1439.

[41] Tavares S. R. et al.: Similarities between Zinc Hydroxide Chloride Monohydrate and Its Dehydrated Form: A Theoretical Study of Their Structures and Anionic Exchange Properties. The Journal of Physical Chemistry C, 118 (2014), 19106–19113.

[42] Garcia-Martinez O. et al.: On the thermal decomposition of the zinc(II) hydroxide chlorides Zn5(OH)8Cl2H2O and ?-Zn(OH)Cl. Journal of Materials Science, 29 (1994), 5429–5434.

[43] Tanaka H. und A. Fujioka: Influence of thermal treatment on the structure and adsorption properties of layered zinc hydroxychloride. Materials Research Bulletin, 45 (2010), 46–51.

[44] Bale C. W. et al.: FactSage thermochemical software and databases, 2010–2016. Calphad, 55 (2016), 1–19.

[45] Tsugita Y.: Problems and Prospects of Halogen Element Contained Dust Treatment in Recycling. MATERIALS TRANSACTIONS, 44 (2003), 2422–2426.

[46] Rösler G. und J. Antrekowitsch: Product Upgrade of Waelz Oxide Using an Alternative Resource. Befesa Steel R&D,

[47] Petar Iliev V. S.: PURIFICATION OF ZINC CONTAINING WAELZ OXIDES FROM CHLORINE AND FLUORINE, University of Chemical Technology and Metallurgy, Sofia, Bulgaria (2016).

[48] DANOBEITIA SIERRA I.: PCT/ES96/00080 – HYDROMETALLURGICAL TREATMENT FOR THE PURIFICATION OF WAELZ OXIDES THROUGH LIXIVIATION WITH SODIUM CARBONATE.

[49] Pawlek F.: Metallhüttenkunde. De Gruyter, Berlin (1983).

[50] Şahin F. Ç., B. Derin und O. Yücel: Chloride removal from zinc ash. Scandinavian Journal of Metallurgy, 29 (2000), 224–230.

[51] Güresin N. und Y. A. Topkaya: Dechlorination of a zinc dross. Hydrometallurgy, 49 (1998), 179–187.

[52] Mats Jansson: Software description Medusa / Hydra.

[53] KTH Stockholm: Hydra / Medusa.

[54] Antuñano N., J. F. Cambra und P. L. Arias: Hydrometallurgical processes for Waelz oxide valorisation – An overview. Process Safety and Environmental Protection, 129 (2019), 308–320.

[55] Kanari N. et al.: Thermal decomposition of zinc carbonate hydroxide. Thermochimica Acta, 410 (2004), 93–100.

[56] Li Z. et al.: Non-isothermal kinetics studies on the thermal decomposition of zinc hydroxide carbonate. Thermochimica Acta, 438 (2005), 102–106.

[57] Huo Y. und Y. H. Hu: Temperature-Induced Irreversible Change of ZnO Optical Energy Gap. Industrial & Engineering Chemistry Research, 51 (2012), 1083–1085.

[58] NICOLL F. H.: Temperature dependence of the emission bands of zinc oxide phosphors. Journal of the Optical Society of America, 38 (1948), 817.

[59] Coogan C. K. und A. L. G. Rees: The Nature of the Thermal Color Change in Zinc Oxide. The Journal of Chemical Physics, 20 (1952), 1650–1651.

[60] Bevan D. J. M., J. P. Shelton und J. S. Anderson: 351. Properties of some simple oxides and spinels at high temperatures. Journal of the Chemical Society (Resumed) (1948), 1729.

[61] van Craeynest F., W. Maenhout-Van Der Vorst und W. Dekeyser: Interpretation of the Yellow Colour of Heat Treated ZnO Powder. physica status solidi (b), 8 (1965), 841–846.

[62] Takahashi H. und K. Tsutsumi: The Structural Change in Zinc Oxide in the Process of Mechanical Treatment. Bulletin of the Chemical Society of Japan, 40 (1967), 7–11.

9 List of figures

10 List of tables

11 Appendix

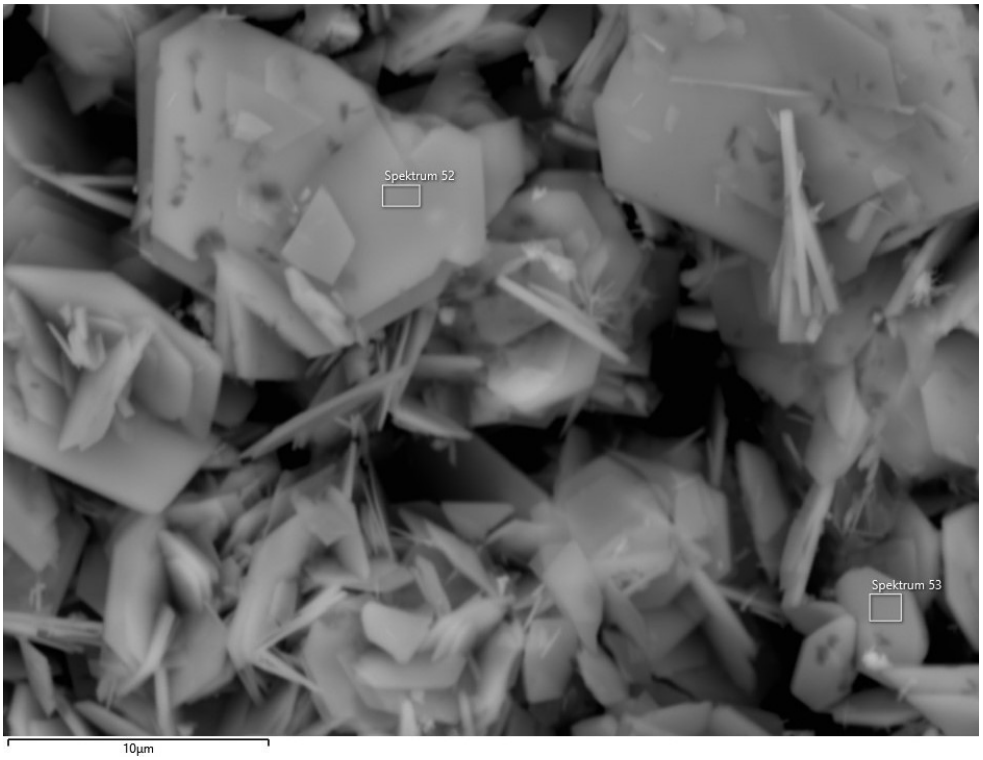

Figure 41: SEM picture of the zinc precipitate from the original route without treatment

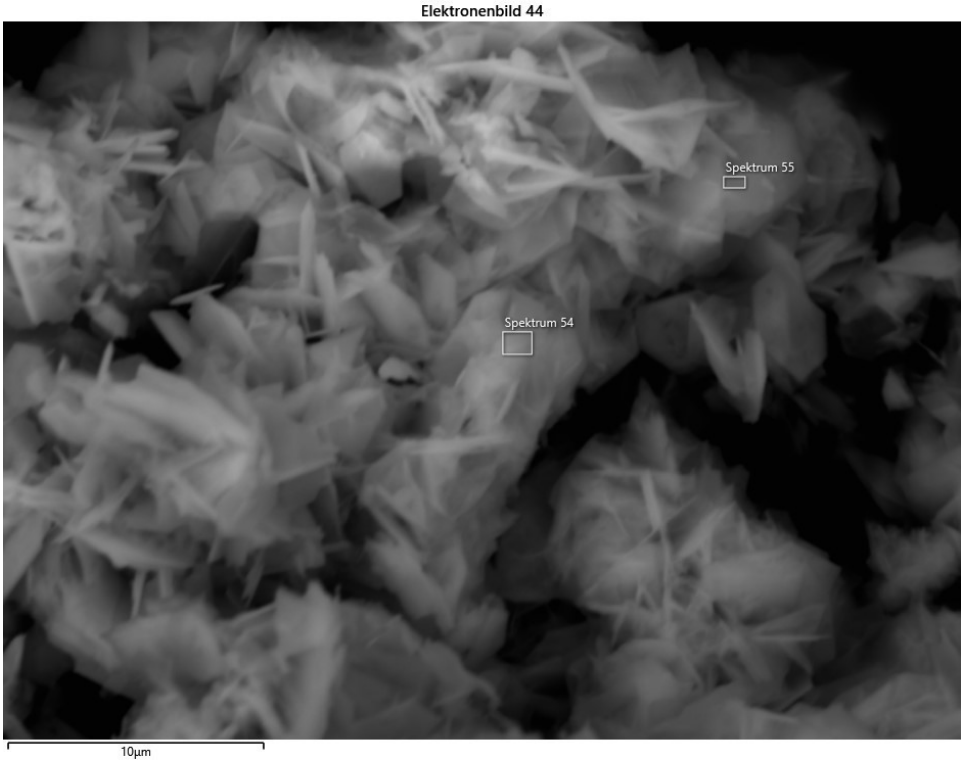

Figure 42: SEM picture of the zinc precipitate from the original route without treatment

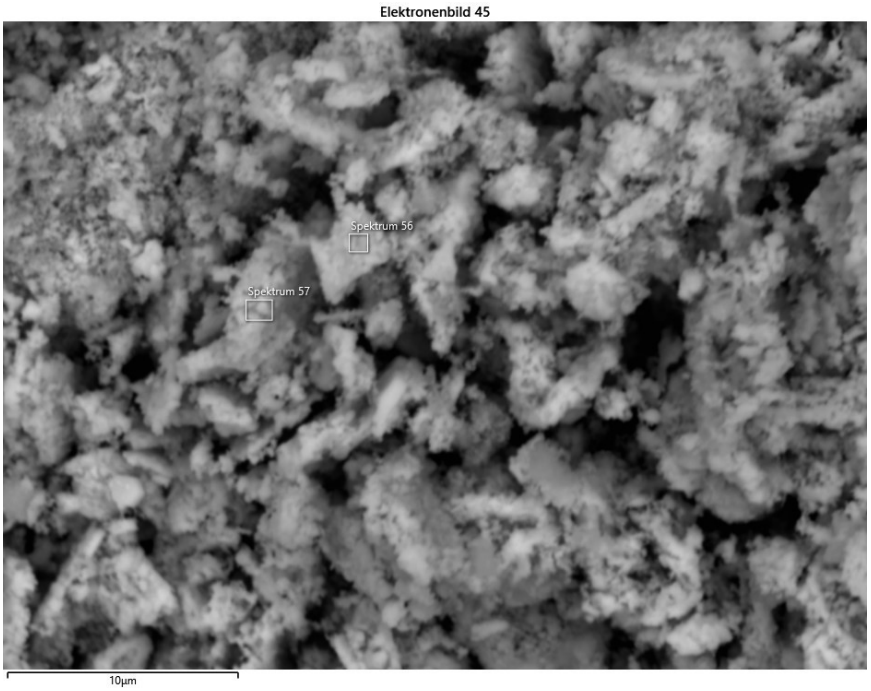

Figure 43: SEM picture of the zinc precipitate after thermal treatment in dry air

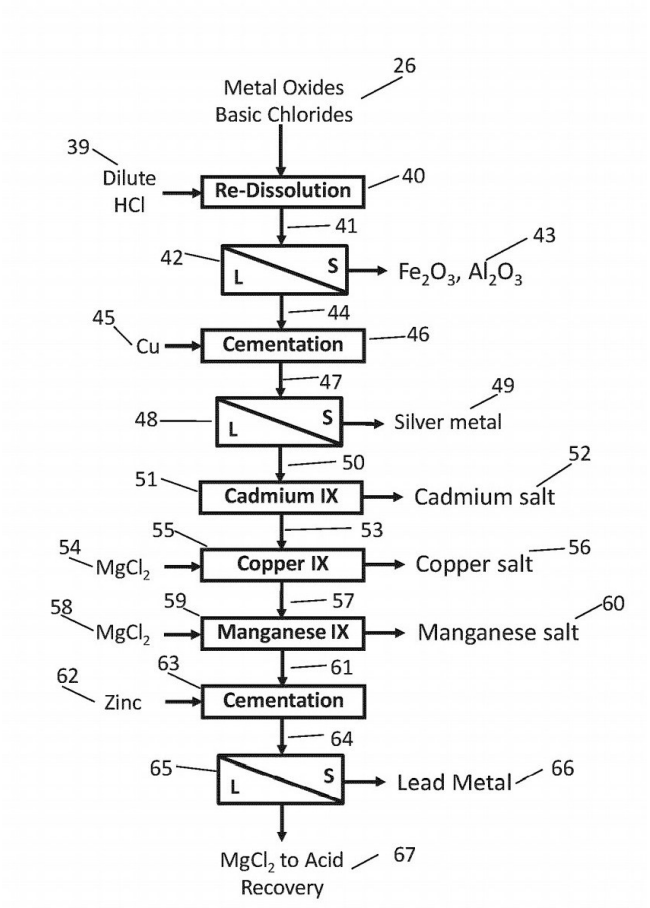

Figure 44: Exemplary further processing of the iron residue for zinc and iron containing input material. Certain steps may vary depending on the actual composition [26]

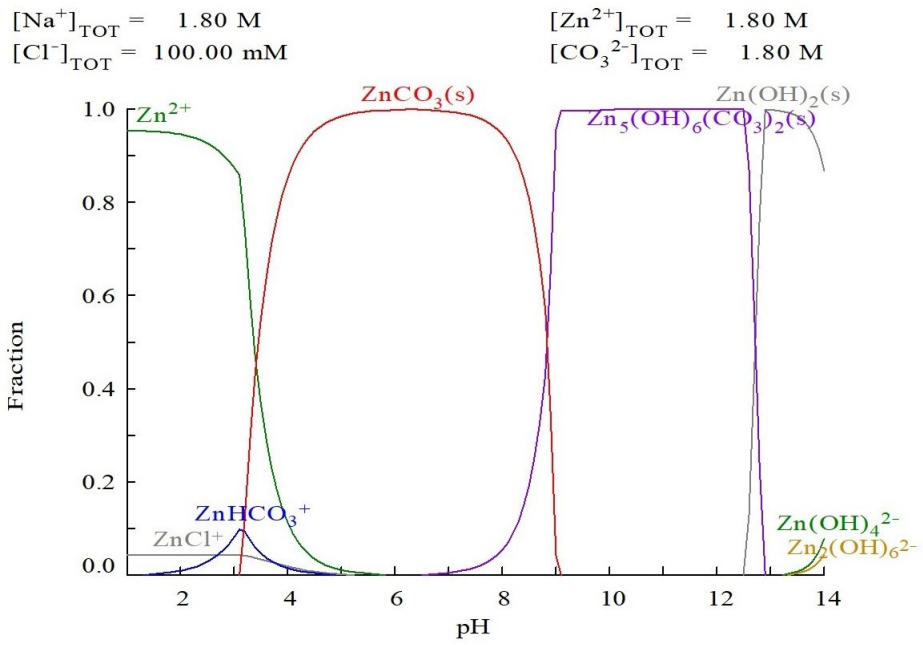

Figure 45: Thermodynamic calculation of the hydrometallurgical treatment with a carbonate content of 0.3 mole per liter [53]

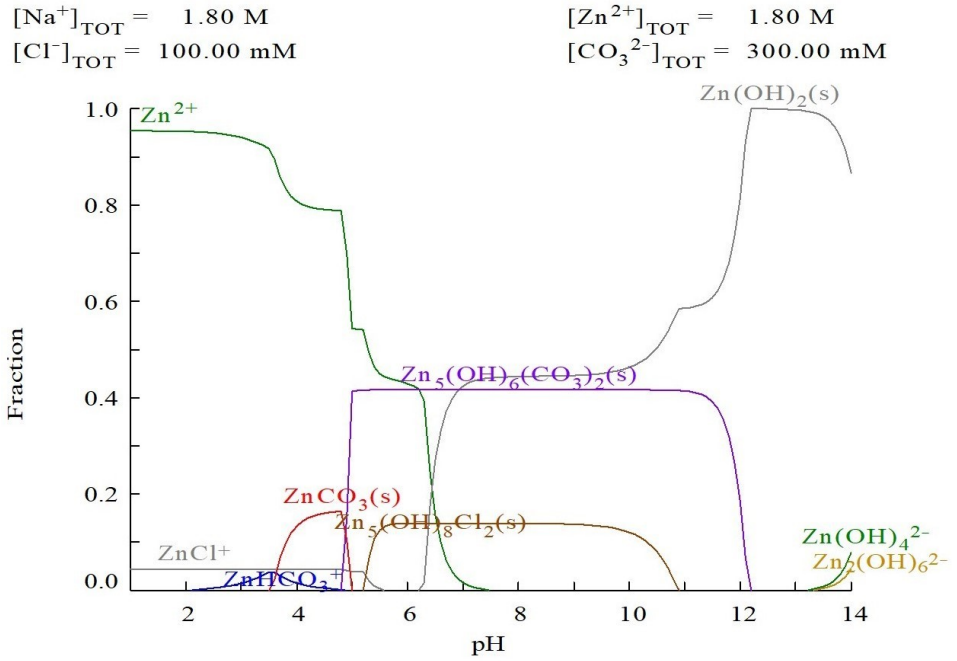

Figure 46: Thermodynamic calculation of the hydrometallurgical treatment with a carbonate content of 0.3 mole per liter [53]

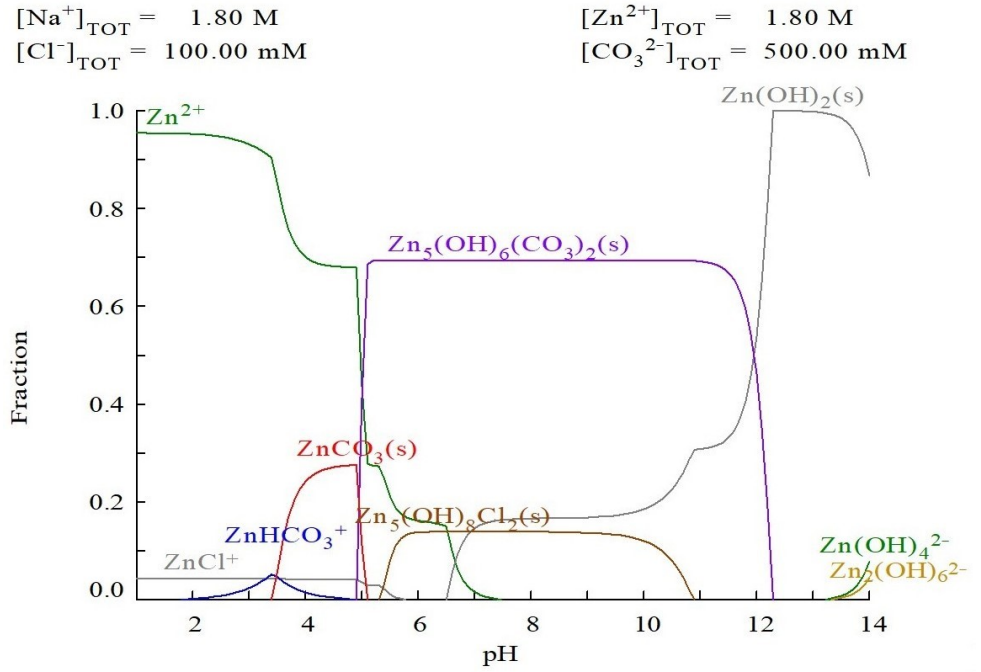

Figure 47: Thermodynamic calculation of the hydrometallurgical treatment with a carbonate content of 0.5 mole per liter [53]

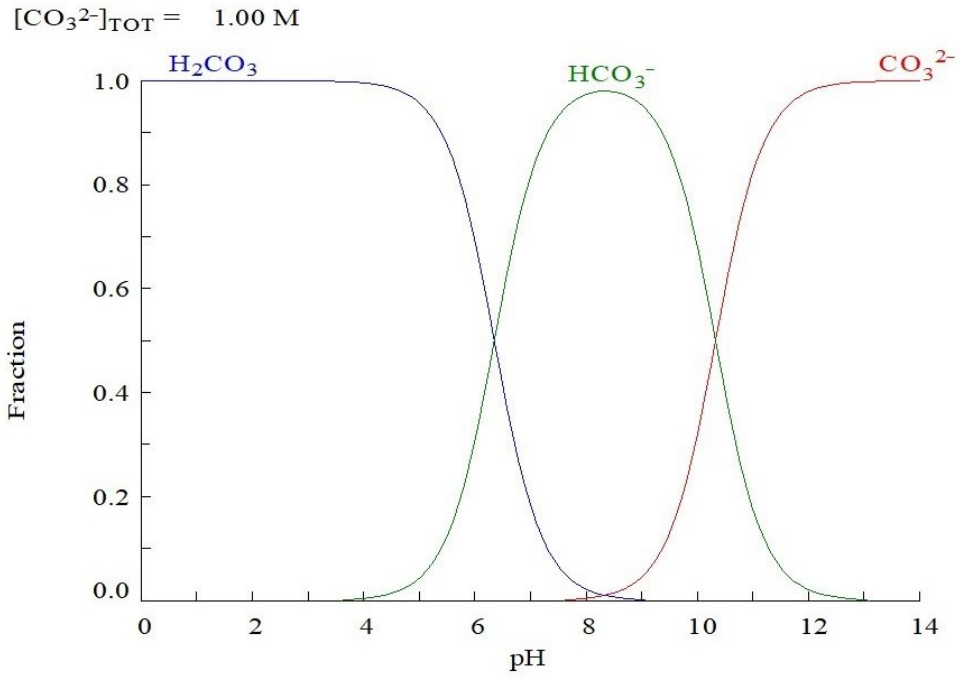

Figure 48: Dissociation of carbonic acid based on the pH level [53]